

2009

Structure of the Swauk formation and Teanaway dike swarm, Washington Cascades

Brigid A. Doran
San Jose State University

Follow this and additional works at: https://scholarworks.sjsu.edu/etd_theses

Recommended Citation

Doran, Brigid A., "Structure of the Swauk formation and Teanaway dike swarm, Washington Cascades" (2009). *Master's Theses*. 3713.
DOI: <https://doi.org/10.31979/etd.5rwr-cdbk>
https://scholarworks.sjsu.edu/etd_theses/3713

This Thesis is brought to you for free and open access by the Master's Theses and Graduate Research at SJSU ScholarWorks. It has been accepted for inclusion in Master's Theses by an authorized administrator of SJSU ScholarWorks. For more information, please contact scholarworks@sjsu.edu.

STRUCTURE OF THE SWAUK FORMATION AND TEANAWAY DIKE SWARM,
WASHINGTON CASCADES

A Thesis

Presented to

The Faculty of the Department of Geology

San José State University

In Partial Fulfillment

of the Requirements for the Degree

Master of Science

by

Brigid A. Doran

August 2009

UMI Number: 1478598

All rights reserved

INFORMATION TO ALL USERS

The quality of this reproduction is dependent upon the quality of the copy submitted.

In the unlikely event that the author did not send a complete manuscript and there are missing pages, these will be noted. Also, if material had to be removed, a note will indicate the deletion.



UMI 1478598

Copyright 2010 by ProQuest LLC.

All rights reserved. This edition of the work is protected against unauthorized copying under Title 17, United States Code.




ProQuest LLC
789 East Eisenhower Parkway
P.O. Box 1346
Ann Arbor, MI 48106-1346

SAN JOSÉ STATE UNIVERSITY

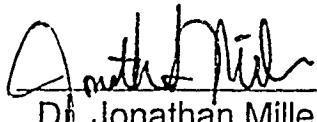
The Undersigned Thesis Committee Approves the Thesis Titled
STRUCTURE OF THE SWAUK FORMATION AND TEANAWAY DIKE SWARM,
WASHINGTON CASCADES

by
Brigid A. Doran

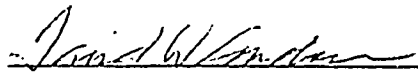
APPROVED FOR THE DEPARTMENT OF GEOLOGY



Dr. Robert Miller, Department of Geology 7 July 2009 Date



Dr. Jonathan Miller, Department of Geology July 1, 2009 Date



Dr. Dave Andersen, Department of Geology 7 July 2009 Date

APPROVED FOR THE UNIVERSITY



Associate Dean Office of Graduate Studies and Research 7/22/09 Date

© 2009

Brigid A. Doran

ALL RIGHTS RESERVED

ABSTRACT

STRUCTURE OF THE SWAUK FORMATION AND TEANAWAY DIKE SWARM, WASHINGTON CASCADES

by Brigid A. Doran

The Eocene Swauk basin and Teanaway dike swarm formed during dominantly regional transtension in the central Washington Cascades, and they give an important view of Eocene shallow-crustal deformation that can be compared with coeval ductile deformation of deeper rocks in the North Cascades crystalline core. The basin is bounded by dextral strike-slip faults and is filled with the clastic Swauk Formation. Shortly after deposition, shortening produced map-scale folds that are broadly similar to those in crystalline rocks. Extension marked by intrusion of the Teanaway dike swarm at ~47 Ma was coincident with roughly similarly oriented dikes that intrude the crystalline core.

Bedding orientations from four transects indicate that the central portion of the Swauk basin was folded three times. The first two generations of gently plunging folds are open to tight, are moderately asymmetrical, have curved hinges, have wavelengths from 0.8-5.8 km, trend northwest to northeast, and accommodated ~26-39% of mainly northeast-southwest shortening. The third generation is a regional, broad, gently southeast-plunging syncline. Teanaway dikes have a mean thickness of 16 m, swing in strike 19° from 216° in the west to 197° in the east, and record ~16-40% arc-parallel to arc-oblique extension. Shortening and extension directions in the Swauk and Teanaway rocks record slight decoupling from Eocene structures in deeper rocks of the Cascades core.

ACKNOWLEDGMENTS

I would like to start by thanking those responsible for bringing me into this world and for the miracle that continues to be my life. This thesis is dedicated to my parents, Tom and Sharon, my sisters, Shay and Ember, and my brother, Burns.

I would also like to give exceptional thanks to my advisor, Dr. Robert Miller, for his undying enthusiasm and patience as well as his guidance and instruction in and outside of the classroom and in the field. He is the one who introduced me to this project and has been pivotal in every step that has led to its success. NSF grant EAR-0511062 funded this project.

I would like to thank my committee members, Dr. Dave Andersen and Dr. Jonathan Miller, for their support and instruction both in and outside of the classroom. Many thanks to my field assistants from San Jose State University, Ante Mlinarevic, Jamie Smith, and Daniel Yokoshima. Special thanks to Ante for enduring those first few weeks and providing insights and laughs. Additional thanks to Jamie and Daniel for their constant encouragement in the field and every day before and since. Finally, I would like to thank Noah McLean and Dr. Joe Vance for their collaboration and help in the field.

TABLE OF CONTENTS

	Page
INTRODUCTION.....	1
Tectonic Setting.....	1
The Swauk Formation and Study Area.....	4
Methods and Purpose.....	9
ROCK UNITS.....	11
Pre-Cenozoic Rocks.....	11
Swauk Formation.....	12
Lateritic Ironstone Deposits.....	13
Sedimentary Serpentinite.....	13
Conglomerate.....	14
Medium-grained Sandstone.....	15
Mudstone-rich Facies.....	18
Teaway Formation and Dike Swarm.....	19
STRUCTURE.....	21
Bed Orientations and Folds.....	23
Intraformational Angular Unconformity.....	36
Overturned Section.....	37
Faults.....	42
Map-scale Shear Zone.....	48
Shortening Analysis.....	51

Teanaway Dikes.....	52
Dike Orientation and Thickness.....	52
Extension.....	59
Contact Relationships of the Swauk Formation.....	61
Contact with the Ingalls Ophiolite.....	61
Contact Between the Swauk Formation and Teanaway Formation.....	64
DISCUSSION.....	65
Bed and Fold Orientations.....	65
Faults.....	72
Nature of Contact between Swauk Formation and Ingalls Ophiolite.....	74
Extension.....	75
Teanaway Dikes.....	75
Analysis of Mean Dike Thicknesses along Transects...	77
Extension and Eocene Dikes Elsewhere in the North and Central Cascades.....	79
Regional Implications.....	81
CONCLUSIONS.....	84
REFERENCES CITED.....	87

LIST OF FIGURES

Figure	Page
1. Generalized Map Emphasizing Eocene Features of Northwest Washington.....	2
2. Relationship of the Swauk Formation to Surrounding Units.....	5
3. Study Region: with Key Locations and Sedimentary Facies.....	7
4. Typical Medium-grained Swauk Sandstones.....	17
5. Typical Teanaway Dike Texture.....	20
6. Generalized Geologic Map Showing Locations of Four Transects.	22
7. Cross-section Along the Cle Elum River Transect.....	24
8. Cross-section Along the Jolly Mountain Transect.....	25
9. Photograph of an Intraformational Angular Unconformity.....	29
10. Cross-section of the Eastern Transect.....	31
11. Lower Hemisphere Projection of Poles to All Beds in the Study Area.....	33
12. Lower Hemisphere Projection of Poles to Beds in the Northern Part of the Cle Elum River Transect.....	34
13. Lower Hemisphere Projection of Poles to Beds in the Southern Part of the Cle Elum River Transect.....	34
14. Lower Hemisphere Projection of Poles to Beds in the Jolly Mountain Transect.....	35

15.	Lower Hemisphere Projection of Poles to Beds in the Eastern Transect.....	35
16.	Location of Short Transect.....	39
17.	Reverse Fault Model for Overturned Strata Along Koppen Mountain Transect.....	40
18.	Normal Fault Model for Overturned Strata Along Koppen Mountain Transect.....	41
19.	Possible Inferred Reverse and Normal Fault Trends.....	43
20.	General Trends of Fold Axes, Dikes, and Faults In and Outside the Study Area.....	45
21.	Geologic Map of Northwest Part of the Study Area.....	46
22.	Deformed Biotite Clasts within Pseudotachylite and/or Ultra- Cataclasite Bands.....	49
23.	Photographs of the Map-scale Shear Zone.....	50
24.	Cartoon Illustrating Shortening Calculations.....	53
25.	Statistical Analysis of Dike Thicknesses Along Transects.....	58
26.	Cartoon Illustrating Extension Calculations.....	60
27.	Geologic Map of Part of the Swauk-Teaway Contact.....	66
28.	Structures in a Typical Wrench Model.....	69
29.	A Portion of the North Cascades Crystalline Core and Adjacent Chumstick and Swauk Basins.....	80

LIST OF TABLES AND PLATES

Table	Page
1. Summary of Fold Data for the Four Transects in the Study Area.	26
2. Compilation of Shortening for the Cle Elum River, Jolly Mountain, and Eastern Transects.....	53
3. Compilation of All Dike Data.....	55
4. Compilation of All Dike Data with Dips $>50^\circ$	58
5. Compilation of Extension Data for the Jolly and Koppen Mountain Transects.....	60
6. Calculations for Maximum Error in Extension Due to the Inclusion of Dikes that Dip $<50^\circ$	60
7. Calculations for Maximum Error in Extension Due to Covered Portions of Transects.....	62
Plate	
1. Structural Map of the Swauk Formation, Central Cascades, Washington	in pocket

INTRODUCTION

The Cascades Range in Washington contains Eocene, non-marine sedimentary basins that are in part bounded by strike-slip faults (Fig. 1) (Johnson, 1984). These basins may be associated with the oblique subduction of the Juan de Fuca plate beneath North America and are considered by most workers to have formed during regional transtension (Johnson, 1984; Tabor et al., 1984; Wells et al., 1984; Johnson, 1985; Evans, 1994). The Swauk basin is one of the oldest of the basins and is noteworthy for its record of rapid subsidence and sediment accumulation (Taylor et al., 1988). Following deposition, the basin was subjected to significant, but poorly quantified, amounts of shortening and then extension. The basin history, from subsidence through shortening, to extension, probably occurred over only about 5 m.y. (Tabor et al., 1982, 1984; Taylor et al., 1988).

Tectonic Setting

Prior to formation of the Swauk basin, the North Cascades experienced mid-Cretaceous (~90 Ma) shortening, crustal thickening, and Barrovian metamorphism (e.g., Misch, 1966; McGroder, 1991; Miller et al., 2006). This regional shortening event was followed by regional transpression from roughly 73 to 55 Ma (Miller and Bowring, 1990; Paterson et al., 2004). Ensuing transtension

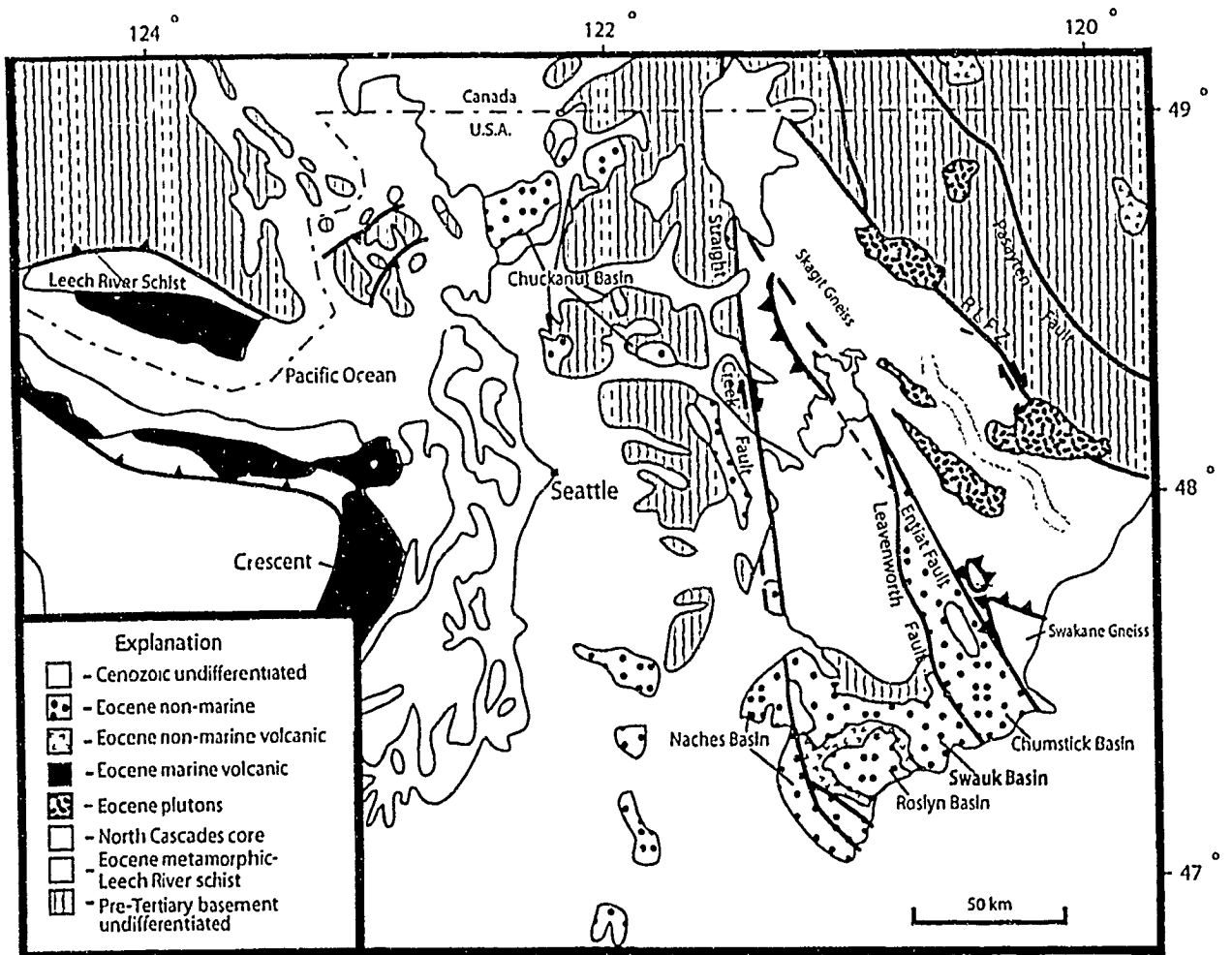


Figure 1. Generalized map emphasizing Eocene features of Northwest Washington. Note Eocene non-marine sedimentary basins adjacent to the Cascades core. Tertiary, right-lateral, strike-slip faults include the Entiat, Leavenworth, Pasayten, and Straight Creek faults and the Ross Lake fault zone (RLFZ).

starting between ~57 and 55 Ma (Miller and Bowring, 1990) in the late Paleocene to early Eocene initiated formation of the Swauk basin and other non-marine basins accompanied by significant exhumation of metamorphic and plutonic rocks of the Cascades core (Tabor et al., 1989; Haugerud et al., 1991; Wernicke and Getty, 1997; Paterson et al., 2004). In sharp contrast to all other workers, Cheney and Hayman (2009) have recently proposed that extension and transtension were not important and that Eocene “basins” are actually structural lows.

Transtension may have resulted from major plate reorganization due to the migration of the triple junction between the Kula, Farallon, and North American plates (Atwater, 1970; Thorkelson, 1995). Engebretson et al. (1985) suggested that transtension was in response to the oblique subduction of the Kula-Farallon ridge, and the ensuing opening of a slab window (e.g., Thorkelson, 1995; Dostal et al., 2003; Madsen et al., 2006; Breitsprecher et al., 2004).

This middle Eocene period of transtension was followed by short-lived transpression (Johnson, 1985; Taylor et al., 1988; Evans and Johnson, 1989) that may have been localized in the region of the Swauk basin and the probably correlative Chuckanut basin (Frizzel, 1979) (Fig. 1). Renewal of transtension in the region was marked by mafic dike swarms and volcanism in the central Cascades, formation of younger middle to late Eocene basins, such as the Roslyn and Chumstick basins, and continued movement on the dextral Straight

Creek fault (Tabor et al., 1984; Johnson, 1985; Evans and Johnson, 1989; Evans, 1994) (Fig. 1).

The Swauk Formation and Study Area

The Swauk Formation fills the elongate, east-west-trending Swauk basin that has a narrow central region and more extensive lobes to the east and west (Fig. 1). The Swauk Formation is an extremely thick (>8000 m) sequence of fluvial, alluvial, and lacustrine deposits (Tabor et al., 1984, 2000; Johnson et al., 1985; Taylor et al., 1988; Evans, 1994; Cheney and Hayman, 2009). In the eastern portion of the basin, the formation has been subdivided into units of voluminous sandstone, conglomerate, shale, and breccia (Taylor et al., 1988). Bedding generally strikes northwest to west-northwest throughout the Swauk Formation (Tabor et al., 1982, 2000). Overtaken sections are found in the central and northern portions of the formation (Tabor et al., 1982, 2000).

The Swauk basin is bounded on the west by the Eocene Straight Creek fault and on the east by the Leavenworth fault (Figs. 1 and 2). The Straight Creek fault has well documented dextral strike-slip (Misch, 1977; Frizzel, 1979; Vance and Miller, 1981; Tabor et al., 1982; Johnson, 1985; Taylor et al., 1988). The Leavenworth fault has documented vertical motion (Evans, 1994; Cheney and Hayman, 2009) followed by dextral strike-slip (Gresens et al., 1981; Evans, 1994). Movement on these faults is inferred to have largely controlled the

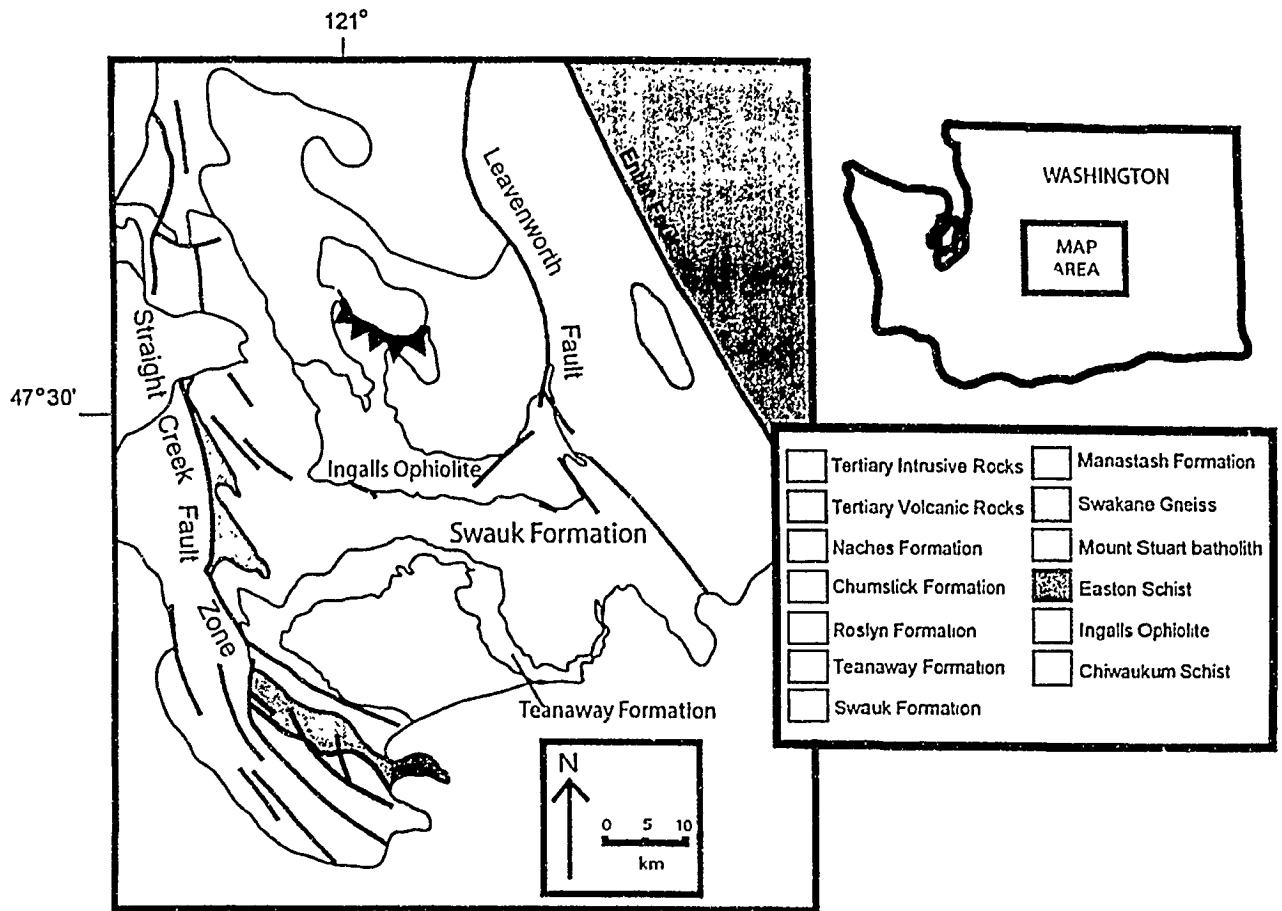


Figure 2. Relationship of the Swauk Formation to surrounding units. Geology modified from Tabor et al. (1982, 1984) and McDougall (1980).

development and depositional patterns of the basin, and possibly the subsequent deformation (Johnson, 1985; Taylor et al., 1988; Evans, 1994).

The study area is located in the central portion of the Swauk basin. This narrow part of the basin is more intensely deformed than the rest of the basin and has received the least amount of previous study. The western boundary of the study area is defined by Lake Cle Elum and the Cle Elum River and extends north to Mount Davis (Fig. 3). The eastern limit is defined by a line that runs north-south through the Miller Creek trailhead (Fig. 3). The northern and southern limits are defined by the contacts of the Swauk Formation with adjacent units.

Several units have been mapped previously in the study area (Fig. 2). The clastic Swauk Formation is the focus of this study. Contact relationships with adjacent units are important for the evolution of the boundaries of the basin and in constraining the style, magnitude, and timing of deformation. The basement of the Swauk Formation in the north is mainly the Jurassic Ingalls ophiolite complex, which is intruded by the 96.5 to 91 Ma Mount Stuart batholith (Tabor et al., 1982, 1987, 2000; Miller, 1985; Matzel et al., 2006), and in the west it is the Easton Metamorphic Suite (Fig. 2). The base of the Swauk Formation is marked by a thin, discontinuous laterite layer that consists of ironstone and reaches 9.75 m in thickness (Lupher, 1944; Lamey and Hotz, 1952; Tabor et al., 1982, 2000). The largely dacitic and andesitic Silver Pass volcanic member (ca. 51 to 52 Ma; N. McLean, written commun., 2006) is intercalated with clastic rocks

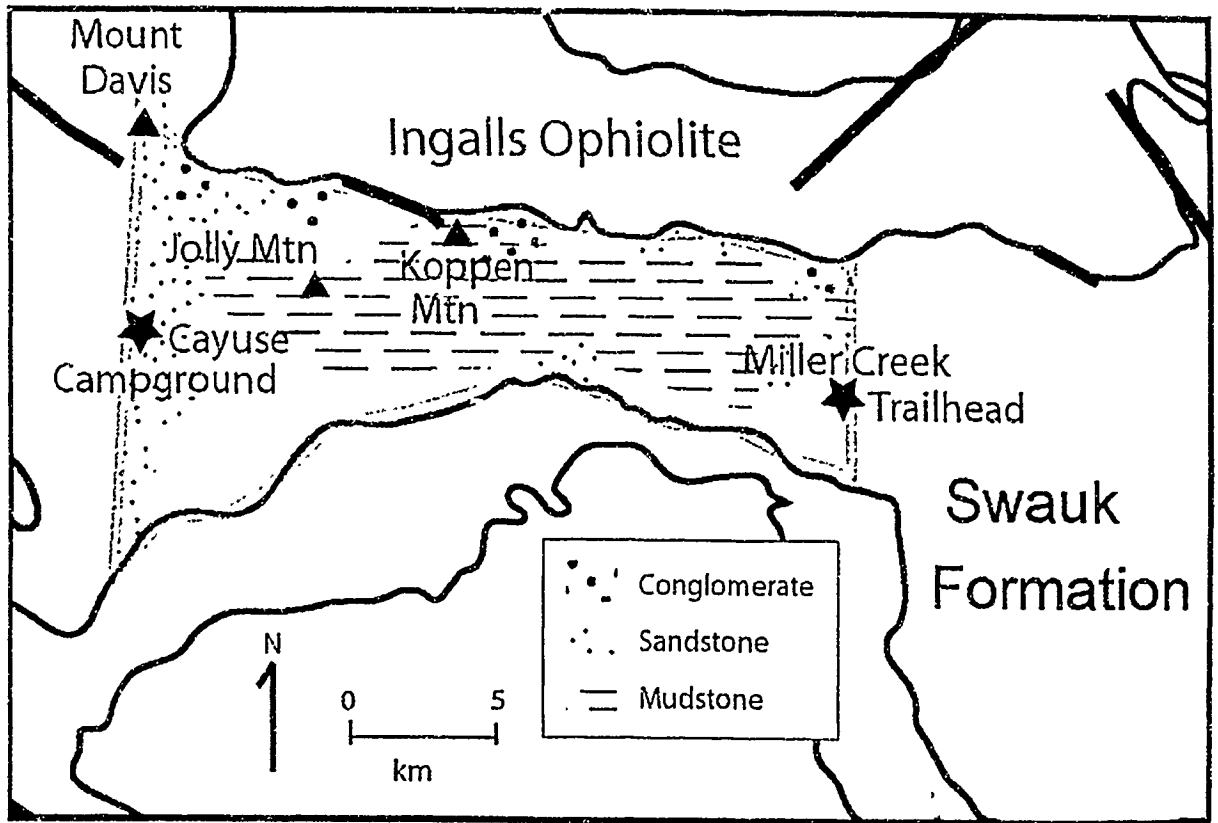


Figure 3. Study region with key locations and sedimentary facies. Study area outlined in red; key locations notated by stars, and mountains by triangles. General location and extent of facies types are illustrated by different textures (see explanation). See Figure 2 for further explanation of units.

in the middle to upper parts of the Swauk Formation (Tabor et al., 1984).

Basaltic flows of the middle Eocene Teanaway Formation (ca. 47 Ma; Tabor et al., 1984) unconformably overlie the Swauk Formation to the south. Diabasic to basaltic Teanaway dikes extensively intrude the Swauk Formation.

The Swauk Formation underwent middle Eocene shortening that preceded eruption of Teanaway volcanic rocks. This shortening produced map-scale folds with axes that have variable, but generally west-northwest trends (Tabor et al., 1982, 1984, 2000). Plunges have not been reported by previous workers. The folds are upright to inclined and generally open, but locally tight (Tabor et al., 1984, 2000). Tight northwest-trending folds have been described west of the study area, adjacent to the Straight Creek fault (Ellis, 1959; Ashleman, 1979). Fold wavelengths gleaned from previously published cross-sections and maps range from 1 to 4 km (Tabor et al., 1982, 2000). Overturned sections imply that unrecognized larger overturned folds may be present. The orientations of previously mapped fold axial traces swing into near-parallelism with the Straight Creek fault as the structure is approached. This is consistent with a classic wrench model (e.g., Wilcox et al., 1973) (Vance and Miller, 1983). Only a few faults have been mapped that cut the Swauk Formation, and no thrust faults have been documented (Tabor et al., 1982, 2000). This is unexpected given the evidence for shortening from folds.

Subsequent extension of the basin is documented by the largely north-northeast-trending Teanaway dikes that cut the Swauk Formation (Smith, 1904;

Foster, 1958). Based on geochemical data, dikes are medium-K tholeiitic basalts and basaltic andesites, thought to have formed in a subduction-zone setting, according to Peters and Tepper (2006), with a mantle source that had been metasomatized as early as 170 Ma (Tepper et al., 2008). The dikes are interpreted to be genetically related, and probably a feeder system, to a large shield volcano and at least some of the flows of the Teanaway Formation (Clayton, 1973). The volcano is located ~6 km west-southwest of the western boundary of the study area. The Teanaway dikes form the largest dike swarm in Washington and are extensional features according to Foster (1958). The dikes presumably track the orientation of the strain field when they were intruded at ~47 Ma. The orientation of dikes is also broadly consistent with a classic wrench-fault model for the Straight Creek fault, as the dikes strike approximately perpendicular to fold axes (Foster, 1958; Johnson, 1985; Taylor et al., 1988) and ~45° to the Straight Creek fault. Prior to this study, there had been no attempt to quantify the orientation of the dikes and the amount of extension they accommodated.

Methods and Purpose

The study area covers >150 km² with variable outcrop exposure. In order to cover the area, four transects across the Swauk Formation and the Teanaway dike swarm were chosen for detailed study. Given the large area, it was not

feasible to trace structures between transects. Orientations of beds (including facing directions), dikes, fold axes, fault slickensides and striae, and shear bands were recorded and interpreted along these transects.

Where feasible, transects were chosen that crossed the strike of structures at a high angle. North-south-trending transects were chosen to examine the structure of the Swauk Formation, whereas northwest-southeast-trending transects were utilized to study the orientations of Teanaway dikes. Cross-sections along the north-south transects helped constrain the minimum amount of shortening of the Swauk Formation. Dike thicknesses along the northwest-southeast transects were used to determine minimum amounts of extension. Statistical analysis was carried out to evaluate variations in average dike widths along dike transects. Textures, modal compositions, and microstructures were determined from 10 sandstone samples of the Swauk Formation and 11 samples of Teanaway dikes.

The overarching purpose of the study is to investigate Eocene shortening and extension at shallow crustal levels in the Washington Cascades. Transpression and transtension in the study area occurred concurrently with deformation of rocks at deeper levels in the Cascades core (e.g. Haugerud et al., 1991; Michels, 2008; Shea, 2008). By comparing extension and shortening directions at deep and shallow levels, the study will evaluate the extent to which the crustal levels were coupled during the Eocene.

In the following, I initially introduce relevant rock units and present petrographic data gleaned from thin-sections. Then, structures in the Swauk Formation are described and structural data for shortening and extension magnitudes and directions are presented. Finally, I discuss interpretations and limitations of these structural data and present the conclusions of the study.

ROCK UNITS

Pre-Cenozoic Rocks

The base of the Swauk Formation is in contact with two units in the study area. Massive serpentinite, sheared serpentinite, and less serpentinitized peridotite of the Jurassic, polygenetic Ingalls ophiolite complex (Miller, 1985; MacDonald et al., 2008) make up most of the basement (Fig. 2). Intercalated greenschist-facies meta-sedimentary and meta-volcanic rocks of the De Roux unit (Miller, 1985) underlie a short segment of the contact. The De Roux unit is poorly dated and is probably Jurassic or late Paleozoic in age (Miller et al., 1993).

Swauk Formation

The Swauk Formation consists primarily of alluvial and fluvial sandstone, mudstone, and conglomerate that are intercalated with minor flows and tuffs of the ~51 to 52 Ma Silver Pass Member (Tabor et al., 1984; N. McLean, written commun., 2006). The Silver Pass Member lies ~4800 m from the base of the Swauk Formation (Tabor et al., 1984) and was observed in two locations, near the northern end of the Cle Elum River transect near Mount Davis and ~6 km south-southeast of Koppen Mountain (Fig. 3). The base of the Swauk Formation is defined by an intermittent lateritic ironstone layer, which is locally overlain by sedimentary serpentinite breccia.

Determination of stratigraphy within the Swauk Formation was difficult and is beyond the scope of this study. However, distinct facies types were recognized and mapped (Fig. 3). The Swauk Formation displays a broad fining upward pattern in the study area. Conglomerates are generally found near the base of the formation. Coarse- to fine-grained sandstones are found throughout the formation, but they are more dominant with proximity to the conglomerates near the base. Mud-rich, silty, fine-grained sandstone is commonly interbedded with medium- to fine-grained sandstone and is dominant in the central portion of the study area at a greater distance from the base of the formation. Facies are generally not laterally continuous for more than ~1500 m.

Lateritic Ironstone Deposits

The basal Swauk Formation is defined by a discontinuous laterite deposit (Lupher, 1944; Tabor et al., 1982, 2000) (Plate 1). The laterite formed from iron-rich soils that developed when the Ingalls ophiolitic complex was subjected to intense tropical weathering at low relief. The laterite reaches a maximum thickness of 9.75 m (Lupher, 1944). Laterite deposits in the study area are massive to pisolitic, black to gray and dark brown with high concentrations of iron. Outcrops are sufficiently magnetic, in places, to deflect a compass needle. A sample examined in thin-section consists largely of magnetite, chrome spinel, and secondary calcite. Many calcite and minor serpentine veins cut the laterite.

Sedimentary Serpentinite

Near El Dorado Creek, in the central part of the study area, sedimentary serpentinite is exposed at the base of the Swauk Formation. The sedimentary serpentinite has a minimum thickness of ~20 m and extends laterally for >100 m. It consists of angular to sub-rounded pebble- to boulder-sized clasts (~5 to ~45 cm in diameter) of serpentinite and peridotite in a fine-grained, yellow, weathered matrix. The sedimentary serpentinite was probably deposited in a high relief environment, was derived from the Ingalls ophiolite, and was transported a very short distance.

Conglomerate

In the study area, outcrop of purely conglomeratic facies is limited. Massive conglomerate was observed at one locality on the western edge of the study area, ~150 m from the contact between the Ingalls ophiolite and Swauk Formation (Fig. 3). The conglomerate extends ~470 m across strike and can be traced >1.5 km along strike from west of the Cle Elum River to the east. At the eastern end, it grades into meter-scale, trough cross-bedded, light, medium-grained sandstone, with pebble conglomerate interbeds. It is matrix supported and has weak planar bedding defined by alignment of the long and intermediate axes of clasts. Clasts are composed largely of serpentinite, peridotite, and biotite granodiorite to tonalite with some metachert and greenstone. The serpentinite, peridotite, and metachert are derived from the Ingalls ophiolite and the granodiorite to tonalite is presumably derived from the Mount Stuart batholith. The well-rounded clasts range in diameter from 1 to 100 cm with a median of 10 cm.

Another thick conglomerate is nearly on strike, ~5 km to the southeast, and may be stratigraphically equivalent to the conglomerate on Cle Elum River (Fig. 3). Beds in the two conglomerates have a similar orientation. The eastern conglomerate has a thickness of ~130 m, cannot be traced along strike because of poor exposure, and is matrix-supported with clasts of biotite granodiorite to

tonalite, vein quartz, and greenstone between 2 and 18 cm in diameter, and with a median of 7 cm.

Minor conglomerate is interbedded with sandstone and mudstone in other locations within ~750 m of the Ingalls contact. These conglomerates occur in beds ranging from a few cm to ~30 cm in thickness. Clasts range from 1 to 18 cm in diameter and have a median of ~4 cm. Plutonic clasts are more abundant east of the major conglomerate on the Cle Elum River. Clasts in the conglomerate on the eastern-most transect are >60% granodiorite to tonalite and biotite gneiss.

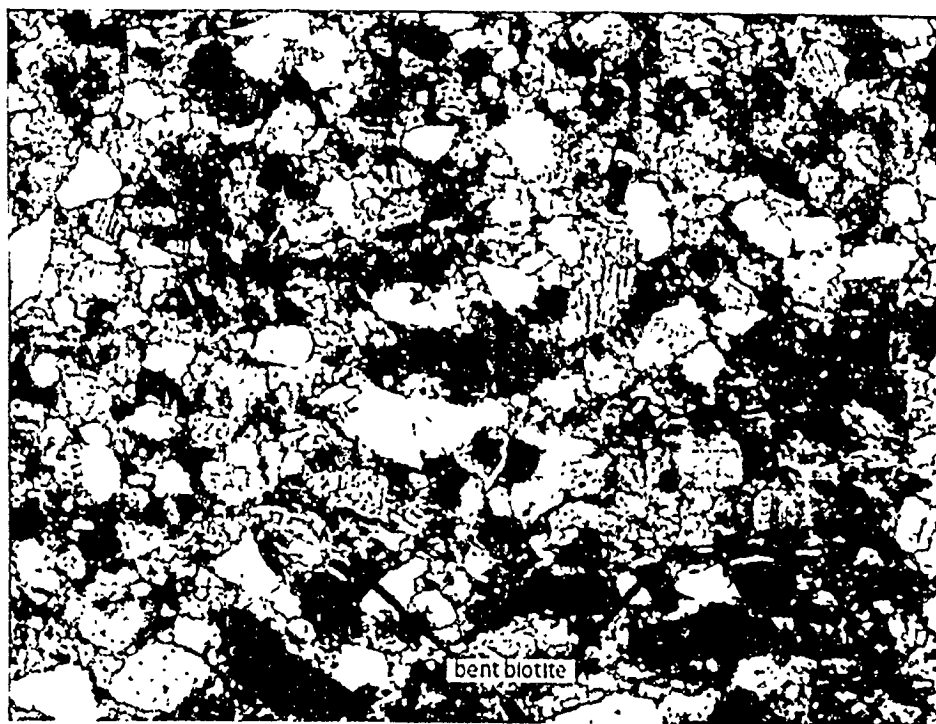
The clasts in the conglomerates are probably derived largely from the nearby Mount Stuart batholith and Ingalls ophiolite. They have been transported or reworked a considerable amount before deposition as the clasts are rounded to subrounded. The conglomerates of the Swauk Formation to the east of the study area have been interpreted as braided river deposits (Taylor, 1985; Taylor et al., 1988).

Medium-grained Sandstone

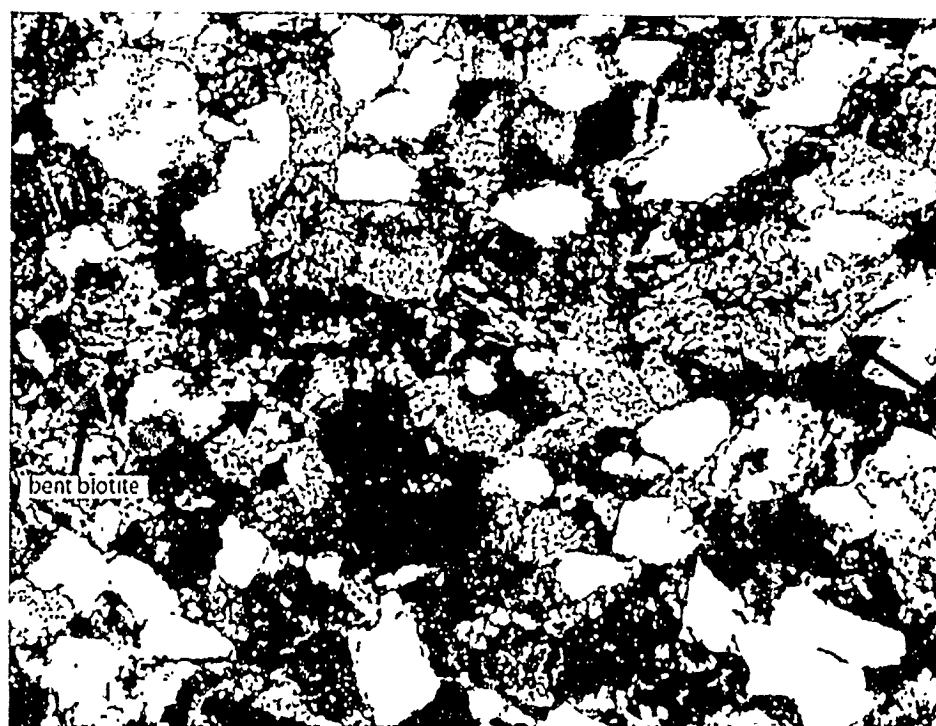
Outcrops consisting solely of massive, coarse- to fine-grained sandstone are rare in the study area and are only found in the western section (Fig. 3). More commonly, medium-grained sandstone is interbedded with mudstone and minor, cm-scale pebble conglomerate layers.

In thin-section, the medium-grained sandstones contain clasts of plagioclase and quartz, with less common biotite and minor muscovite; micas range from <3% to 15%. Typical modal percentages of quartz are 43% with a range of 25% to 70%. Modal percent plagioclase is typically 27%, but ranges from 15% to 40%. Rock fragments range from 3% to 30%, and potassium feldspar is largely absent (Fig. 4). Rock fragments include phyllite and mica schist, poly-crystalline metamorphic quartz, medium- to fine-grained ophiolitic basalt, and fine-grained granodioritic to tonalitic fragments. Mineral accessories include epidote, sphene, chlorite, serpentine, hornblende, and garnet. Some chlorite and epidote are secondary to biotite and plagioclase, but they are also found as primary clasts.

Grains range in diameter from 0.03 mm to 1.4 mm with a median of ~0.5 mm. The sandstones are largely grain supported with moderately- to well-sorted and sub-angular to sub-rounded clasts. Bedding is microscopically defined by alignment of micas, chlorite, opaque grains, and foliated metamorphic rock fragments. Deformation is consistently recorded by micas from sample to sample. The micas are kinked, folded, and less commonly wrapped around other grains (Fig. 4). This deformation probably resulted from compaction during diagenesis.



1 mm



1 mm

Figure 4. Typical medium-grained Swauk sandstones. Sandstone is grain-supported, with high quartz and feldspar content, and bent biotite and foliated metamorphic rock fragments.

Mudstone-rich Facies

Minor amounts of muddy siltstone to silty mudstone and shale are interbedded with sandstones and conglomerates throughout the Swauk Formation. There is also a >28 km² area in the central portion of the study area where the abundance of mudstone exceeds that of coarser-grained rocks. Near Koppen Mountain, the mudstone makes up >70% of the exposed Swauk Formation and is >3 km thick. Across strike, the Swauk Formation south of Jolly Mountain is composed of $\geq 50\%$ mudstone. The facies likely extends >6 km between Jolly Mountain and Koppen Mountain, and possibly extends >23 km from west to east across the entire middle to southern portion of the study area (Fig. 3).

The mudstones are either dark gray to dark brownish-gray or light tan to white. Outcrops are finely laminated and cleave along bedding planes. Laminations can be planar, crenulated, or rippled. Soft-sediment deformation is common, including mm- to cm-scale flame structures due to loading, convolute bedding with amplitudes of <3 cm, and fluid escape structures, such as dish and pillar structures that disrupt up to 4 cm of laminated layers.

Teanaway Formation and Dike Swarm

The middle Eocene (~47 Ma; Tabor et al., 1984) Teanaway Formation consists predominantly of subaerial lava flows that are mostly basalts, but range to rhyolites. Tuffs and breccias are common, as well as minor feldspathic sedimentary rocks (Tabor et al., 1984, 2000). South of the Jolly Mountain transect, the Teanaway Formation consists of basaltic flows, green and red tuffs with secondary calcite in vugs, and monolithologic volcanoclastic breccias.

The dikes most commonly intrude the Swauk Formation, but also intrude adjacent older units. Individual dikes range from basalt to diabase. In hand sample, the dikes exhibit considerable variety. The majority resemble unaltered, dark, fine-grained basalt, but others are coarser-grained and range in color from tan to greenish-gray. Hand samples are inequigranular to mildly porphyritic with large laths of plagioclase. In thin-section, the dikes appear to be compositionally more consistent. They have a predominantly inequigranular to porphyritic, subophitic, diabasic texture. In addition to plagioclase, the dikes contain abundant clinopyroxene, lesser concentrations of opaque phases, and fewer hornblende crystals, as well as secondary epidote (Fig. 5). Most samples contain secondary chlorite, and a few contain secondary biotite and calcite. A few of the dikes contain numerous highly elongate apatite crystals, which suggests quenching (e.g., Winter, 2001).

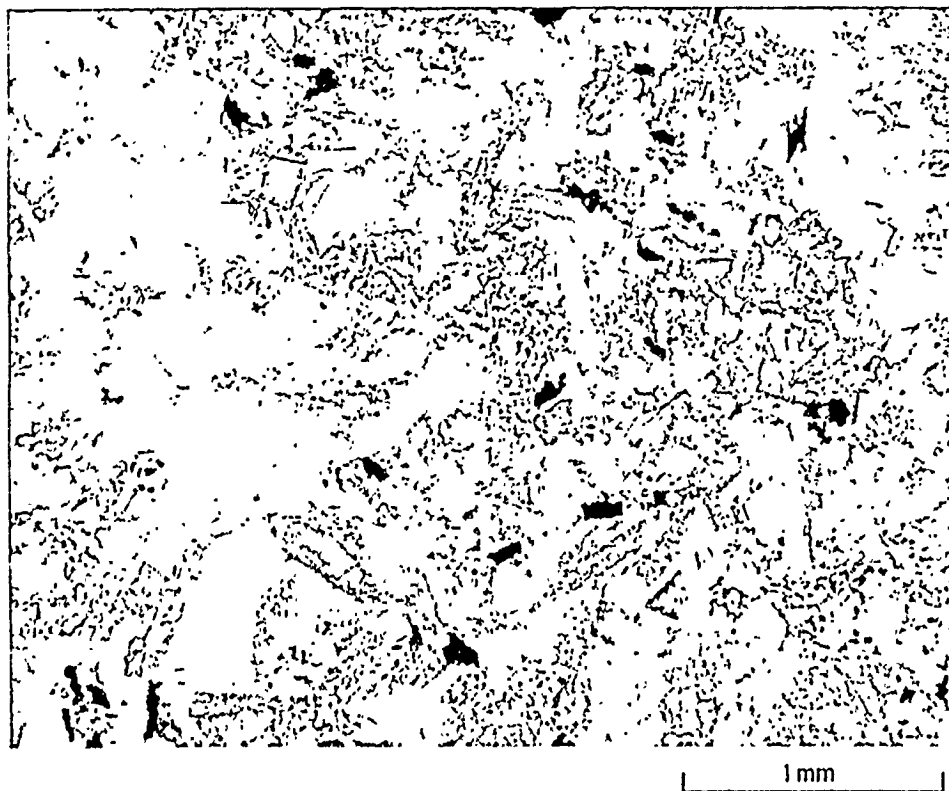


Figure 5. Typical Teanaway dike texture. Dikes are subophitic, inequigranular, and diabasic with plagioclase and clinopyroxene. Top image in crossed nicols and bottom in plane-polarized light.

STRUCTURE

Structures in the study area include map-scale to meter-scale folds, brittle-ductile shear zones and brittle faults. Widespread dikes and at least one angular unconformity are also present. Structural trends in the Swauk Formation are generally northwest-southeast to nearly east-west, whereas Teanaway dikes strike northeast-southwest.

Four major transects were completed across the Swauk basin. From west to east, they are: the Cle Elum River transect, Jolly Mountain transect, Koppen Mountain transect, and Eastern transect (Fig. 6). Due to the different orientations of the transects and structural trends in the Swauk Formation and Teanaway dike swarm, individual transects were chosen to study different structural elements; some transects are oriented nearly perpendicular to the dominant strike of the Teanaway dikes, whereas others are at a high angle to beds in the Swauk Formation. The Cle Elum River transect and Eastern transect run north-northeast-south-southwest to nearly north-south, and bed orientations and analysis of shortening in the Swauk Formation were the focus of these transects. Cross-sections were constructed along these transects and the Jolly Mountain transect. The Jolly Mountain transect and Koppen Mountain transect trend north-northwest-south-southeast to northwest-southeast. Dike orientations and analysis of extension were thus the concentration for these transects.

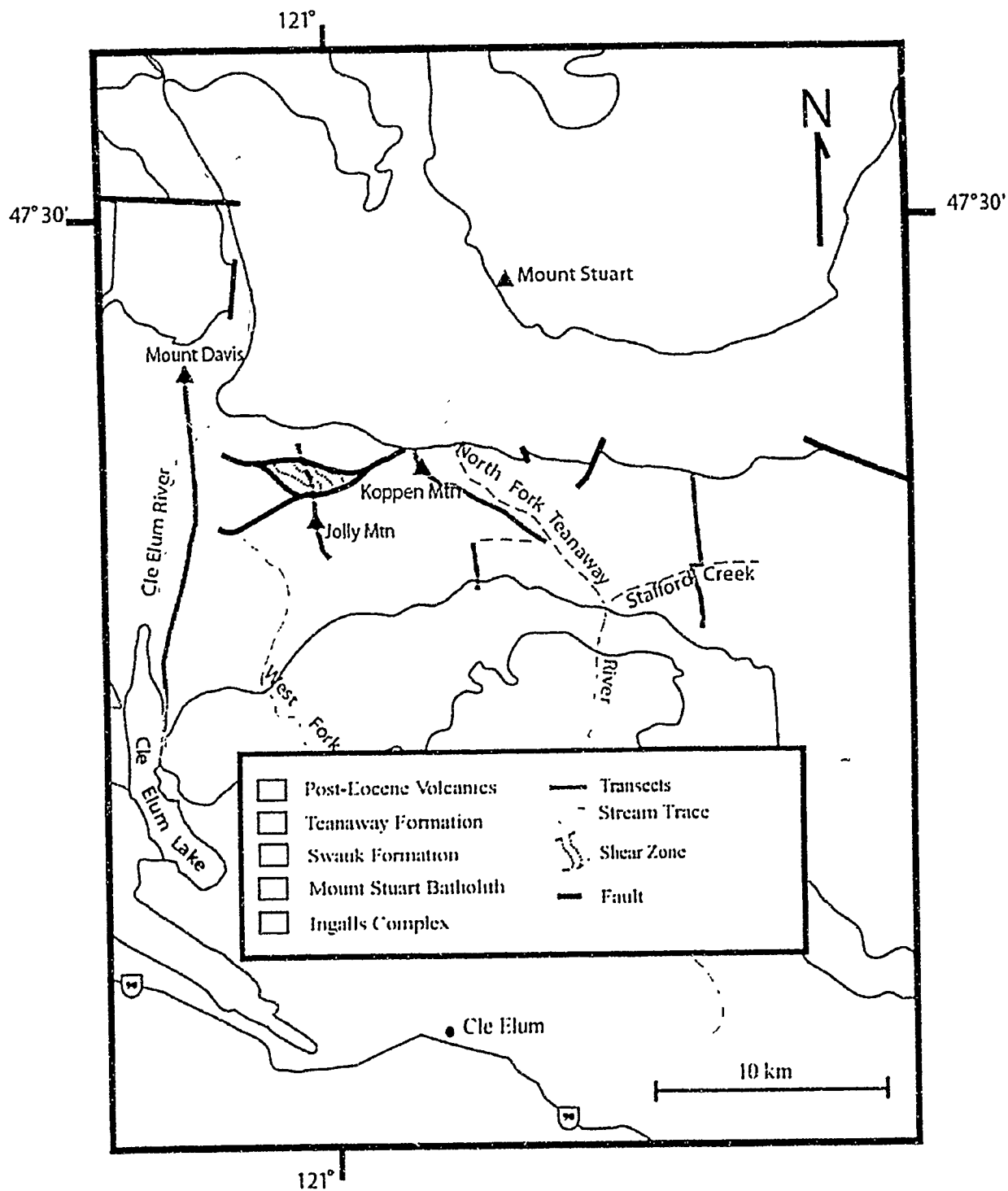


Figure 6. Generalized geologic map showing locations of four transects. Geology modified from Tabor et al. (1982a, 1984) and McDougall (1980).

Bed Orientations and Folds

The entire Swauk Formation has undergone shortening, which produced map-scale to meter-scale folds. Folds are upright to inclined with variable vergence from transect to transect and along individual transects. Dips of axial planes range from vertical to 35° . Folds are open to locally tight, and interlimb angles are generally $\sim 100^\circ$, but range from 15° to 165° . Hinges are rounded and wavelengths range from <5 m to >5 km (Figs. 7 and 8). There is no evidence for thickening of beds, ductile flow towards hinges, or formation of axial-planar cleavage. These observations, combined with the inferred shallow depths of deformation, lead to the interpretation that folds formed by flexural-slip.

Along each transect, the locations of fold hinges were interpreted from dip reversals and/or changes in facing direction (Plate 1). Fold axial planes, wavelengths, amplitudes, and interlimb angles were interpreted from cross-sections. Results are in Table 1.

The Cle Elum River transect is ~ 14 km long (Fig. 7). In the north, beds are primarily gently to moderately (15° - 61°), southwest- to west-dipping. Fold hinge lines plunge gently to the northwest. Axial planes of four folds are steeply north-northeast-dipping (average of 73° , range of 60° - 88°) and wavelengths average 1000 m and range from 840 m to 1224 m. Amplitudes of folds for this portion of the transect average 456 m and range from 432 m to 480 m, and

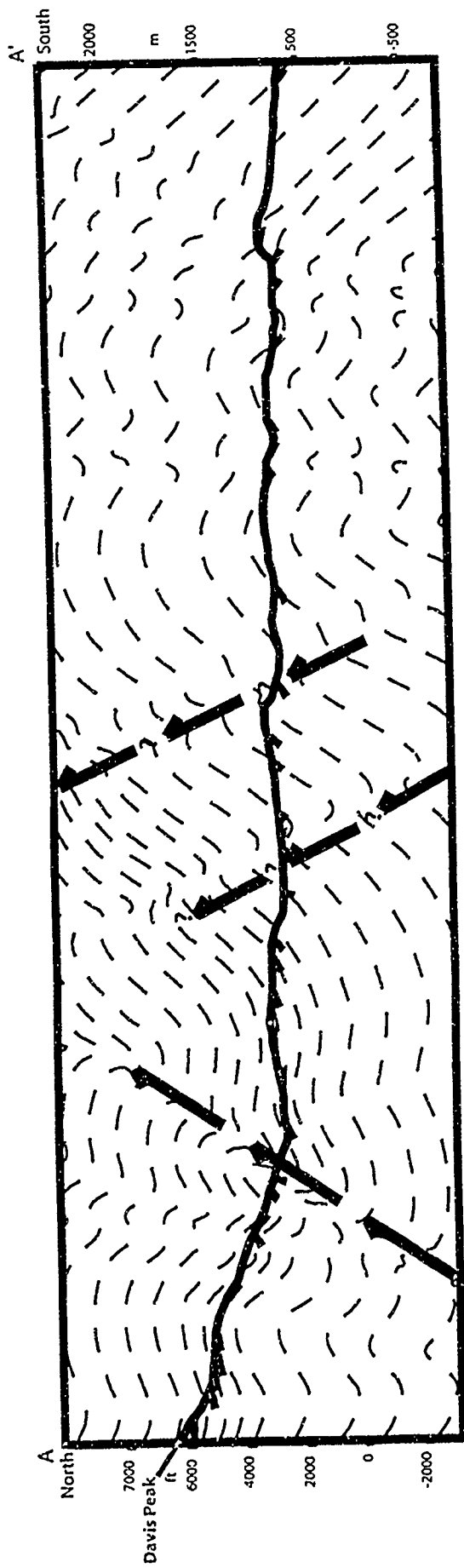


Figure 7. Cross-section along the Cle Elum River transect. Red dashes represent traces of measured beds and half arrows represent inferred thrusts (See Fig. 6 and Plate 1 for location). The transect is made up of large north-west-trending folds and smaller folds that have east-northeast trending axes. No vertical exaggeration.

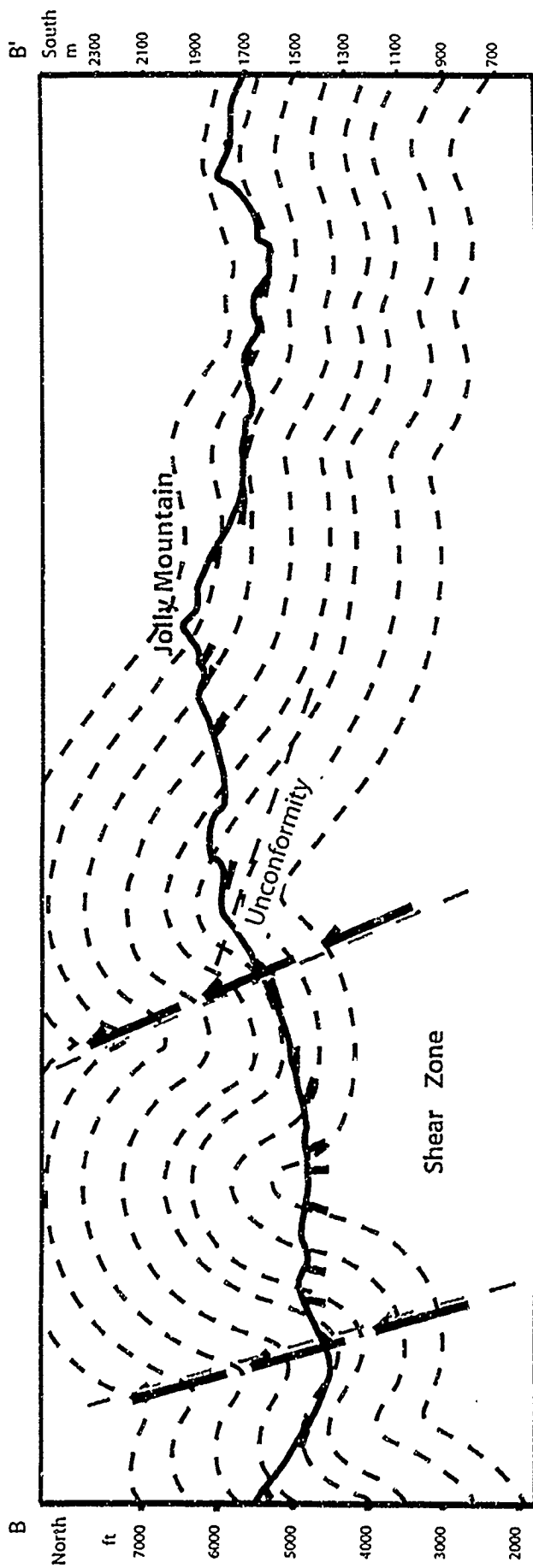


Figure 8. Cross-section along the Jolly Mountain transect. Red dashes represent traces of measured beds, green dashed lines outline the map-scale shear zone, and the blue dashed line represents the location of the intraformational angular unconformity (See Fig. 6 and Plate 1 for location). The transect is made up of one large northwest-trending anticline and smaller folds that have east-northeast trending axes. No vertical exaggeration.

Table 1. SUMMARY OF FOLD DATA FOR THE FOUR TRANSECTS IN THE STUDY AREA.

Transect	Section	Beds			Large folds					Small-scale folds							
		dip		degree facng	hinges		dip of axial planes			hinges		dip of axial planes					
		direction	SW-W		NE	11-64	trend	plunge	d.rection	degree	wavelength (m)	amplitude (m)	interlimb angle(°)	trend	plunge	d.rection	degree
Cla Elum	north	SW-W	15-61		NW-WW	NNE	73	1000	456	75	W-SW	SW-SSE	74	1600	105	127	
	central	NE	11-64								W-SW	NNW-NE	78	776	84	140	
	south	SSE	10-65														
Joly Mountain	south+central				NW		5800	1700									
	north	NW	31-89		NW-W	SSW	85	1300	160	65							
	central	S	05-43		WNW	SSW	80	1900	336	80							
Koppen Mountain Eastern	south	S	14-28	upright		NNE	80	1500	72	140							
	entire	NNE	61-90	overturned													
	north	S	69-81	upright	ENE	NNW	87	1100	300	37	E-ESE	NNW	43	972	312	92	
	south+central	S	44-75														

interlimb angles average 75° and range from 50° to 98° (Table 1). The central section of the Cle Elum River transect has primarily moderately to gently (11° - 64°), northeast-dipping beds that form the north-dipping limb of a large, northwest-trending, asymmetric anticline that has a wavelength of ~ 5.8 km and amplitude of ~ 1.7 km (Fig. 7 and Plate 1). There are three smaller folds that have hinge lines trending west-southwest to northwest with steeply southwest to south-southeast-dipping axial planes (average of 74° , range of 65° - 86°). The smaller folds have wavelengths that average 1.6 km and range from 960 m to 2400 m, amplitudes that average 105 m and range from 60 m to 168 m, and interlimb angles that average 127° and range from 108° to 150° . The southern section of the Cle Elum River transect has primarily moderate to gently (10° - 65°), south-southeast-dipping beds that form the hinge zone and south-dipping limb of the large anticline. There are six smaller folds in this section (Fig. 7 and Plate 1). They have nearly west- to southwest-trending hinge lines and steeply north-northwest to northwest-dipping axial planes (average of 78° , range from 68° - 86°). These smaller folds have wavelengths that average 776 m and range from 600 m to 960 m, amplitudes that average 84 m and range from 36 m to 168 m, and interlimb angles that average 140° and range from 134° to 147° (Table 1). In summary, the entire Cle Elum River transect has small and larger-scale folds that are both north- and south-vergent with hinge-line orientations ranging from east-west to northwest in the north and southwest in the south. Beds are generally gently to moderately dipping and have highly variable orientations.

The Jolly Mountain transect (Fig. 8) is ~6 km long. The northern section crosses a 1.2-km-wide zone of intense shear marked by grain-size reduction, abrupt changes in bedding on the meter scale, development of cm-scale shear bands, and pervasive fracturing. On a larger scale, north of the shear zone, beds dip 31° to 57° with variable orientations. Beds steepen to between 60° and 89° within the shear zone and shallow to between 06° and 43° south of the shear zone (Plate 1). At least two large folds have northwest- to nearly west-trending hinge-lines with steep (82° and 88°) south-southwest-dipping axial planes. Wavelengths are 1.2 km and 1.4 km, amplitudes are 216 m and 108 m, and interlimb angles are 52° and 80°, respectively (Table 1). An intraformational angular unconformity with $\geq 21^\circ$ of discordance, as interpreted from photographs (Fig. 9), is exposed in the central part of the transect. South of the unconformity, there are primarily gently (6° to 43°) south-dipping beds that form the south limb of an asymmetric anticline with a short, steep, north-dipping limb (Fig. 8). The hinge line trends west northwest and plunges gently, the axial plane dips steeply (~80°) to the south-southwest, the wavelength is ~1.9 km, the amplitude is ~336 m, and the interlimb angle is ~80° (Table 1). The southern section of the Jolly Mountain transect has two smaller folds that have steep to vertical (87° and 90°), slightly north-northeast-dipping axial planes. Their wavelengths are 1.3 km and 1.8 km, amplitudes are 36 m and 108 m, and interlimb angles are 133° and 146° (Table 1).



Figure 9. Photograph of an intraformational angular unconformity. The unconformity is in interbedded sandstone and mudstone of the Swauk Formation on the eastern flank of Jolly Mountain. The unconformity shows a minimum of 21° of discordance as viewed from the east. Beds above the unconformity dip away and steepen, ending at the southern end of the Jolly Mountain transect as the steep limb of an asymmetric anticline.

The Koppen Mountain transect is ~8 km long and represents an apparent stratigraphic thickness of >3600 m. The entire transect consists of steeply (61° to 90°) north-northeast-dipping, overturned beds. The orientations of 48 beds were measured; 23% of these beds have facing indicators and all are overturned, in agreement with observations of Tabor et al. (1982). Facing was determined from onlap and scour surfaces of ripples, loading structures, and fluid escape structures in the mudstone-rich facies.

The Eastern transect is 4 km long. The northern part of the transect consists of primarily steep (68° to 81°), south-dipping, upright beds (Fig. 10, Table 1, and Plate 1). One large fold has an east-northeast-trending hinge line with a steep (87°) north-northwest-dipping axial plane. The wavelength of this fold is 1.1 km, the amplitude is ~300 m, and the interlimb angle is ~37° (Table 1). The central and southern sections of the Eastern transect consist of primarily moderately to steeply (44° - 75°), south-dipping beds with a small fold on the south limb of an anticline. The axial plane of this fold is gently (43°) north-northwest-dipping. This fold has a wavelength of 972 m, amplitude of 312 m, and an interlimb angle of 92° (Table 1).

The orientation of the fold axes in the study area is utilized to determine the shortening direction recorded by folds. Few fold hinges were sufficiently exposed for measurement in the field and axes were thus determined utilizing stereographic projections and cross-sections. The analysis of stereographic

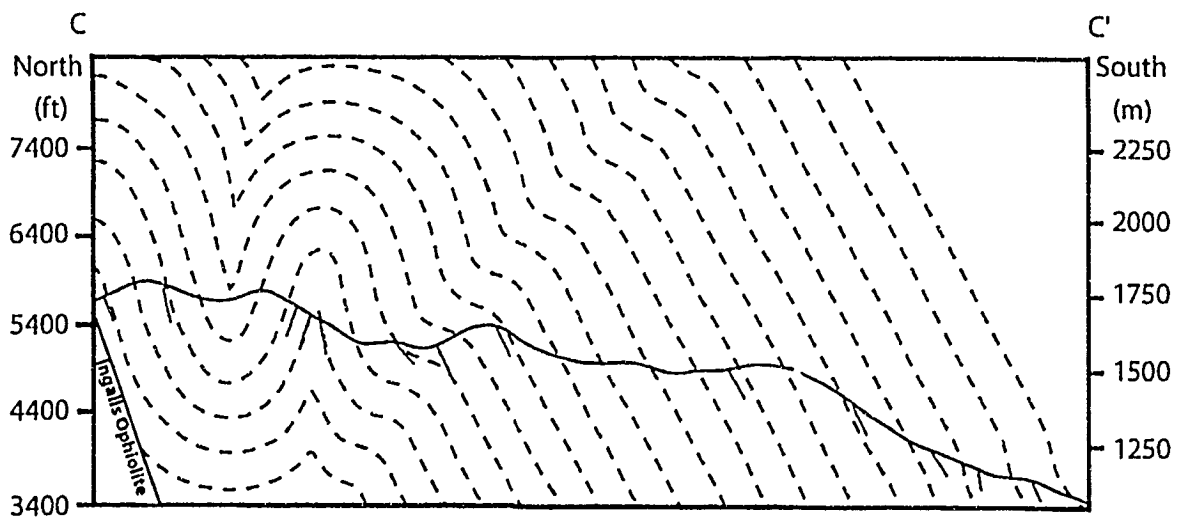


Figure 10. Cross-section of the eastern transect. The red dashes represent the traces of measured beds (See Plate 1 for location). No vertical exaggeration.

projections also allows for interpretation of cylindricity and shape of folds for different transects. Pi axes determined from the poles to bedding measurements for the whole study area show that the average orientation of fold axes is 08/104° (Fig. 11). There is a high degree of scatter from the girdle, however, which indicates that, at the scale of the study area, folds are highly non-cylindrical. Fold shape, cylindricity, and axes calculated for individual transects from stereographic projections also show significant variability.

The pi axis for the Cle Elum River transect is oriented 05/113°. Pi axes vary modestly for different parts of the transect; they are oriented 02/298° in the north (Fig. 12) and 15/105° in the south (Fig. 13). In the north, folds appear to be asymmetric and the high degree of scatter from the girdle indicates that folds are highly non-cylindrical. It is possible to draw a second, less well defined, pi axis at ~15/260° (Fig. 12), which supports the existence of high variability of fold orientations. In the south, folds also appear to be asymmetric; there is only moderate scatter of points off the girdle and folds are thus more cylindrical (Fig. 13).

The pi axis calculated for the Jolly Mountain transect is oriented 12/109° (Fig. 14). Folds are asymmetric and the poles to beds have a moderately high degree of scatter from the girdle indicating moderately low cylindricity (Fig. 14).

The pi axis for the Eastern transect is oriented 52/221° (Fig. 15), but data do not appear to fit any statistically meaningful girdle. Dip reversals and cross-sections show that the majority of bedding measurements were collected on the

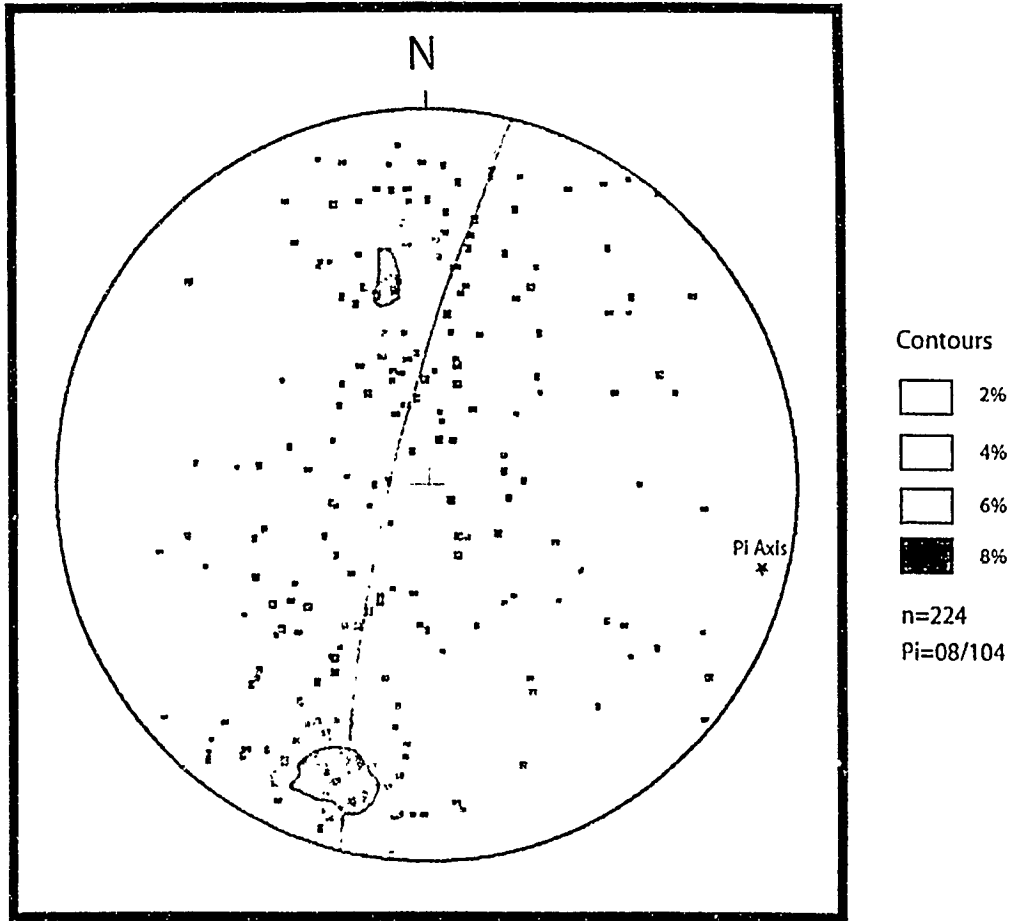


Figure 11. Lower hemisphere projection of poles to all beds in the study area.

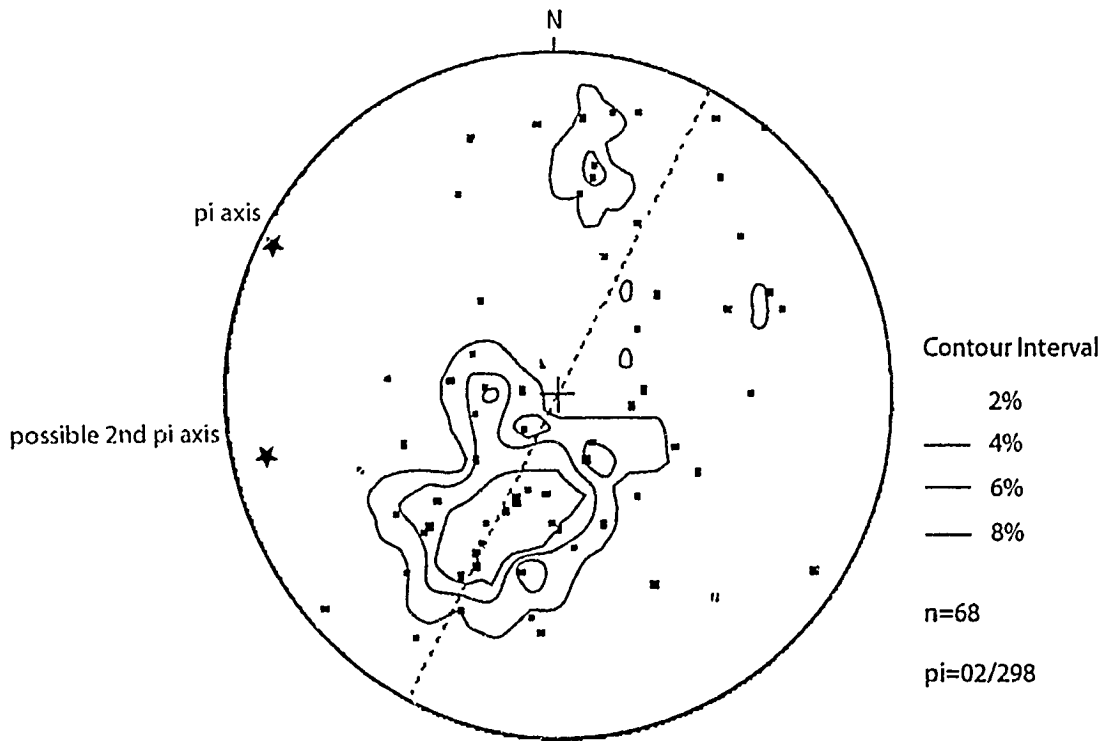


Figure 12. Lower hemisphere projection of poles to beds in the northern part of the Cle Elum River transect. Projection produced using GEORient 9.2.

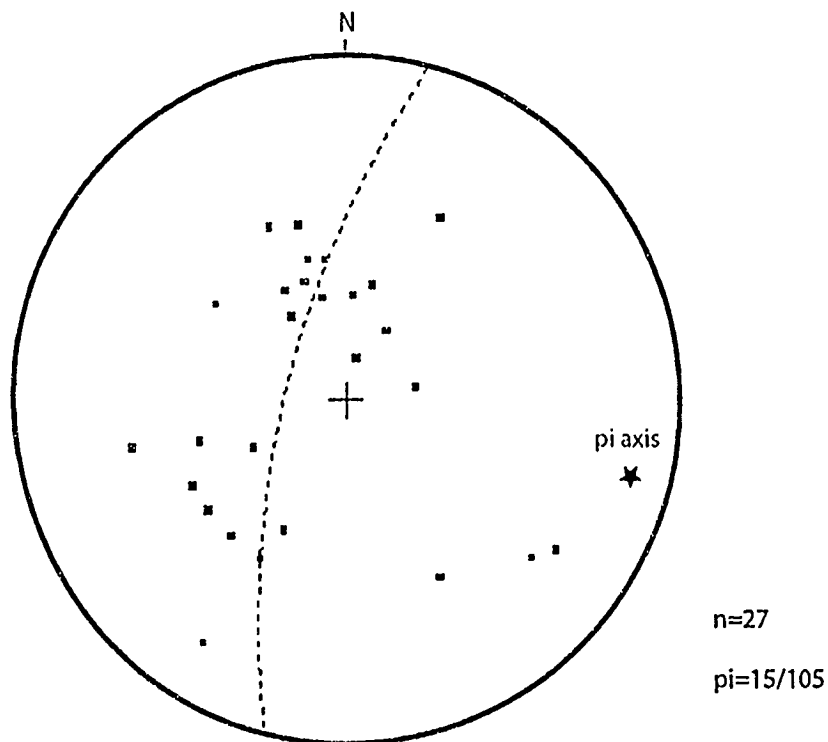


Figure 13. Lower hemisphere projection of poles to beds in the southern part of the Cle Elum River transect. Projection produced using GEORient 9.2.

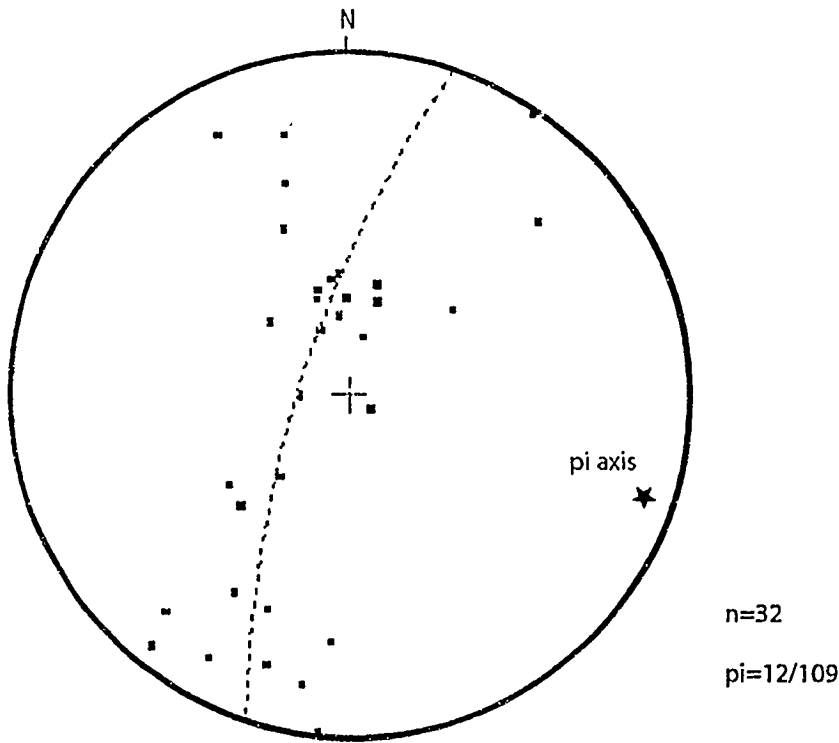


Figure 14. Lower hemisphere projection of poles to beds in the Jolly Mountain transect. Projection produced using GEORient 9.2.

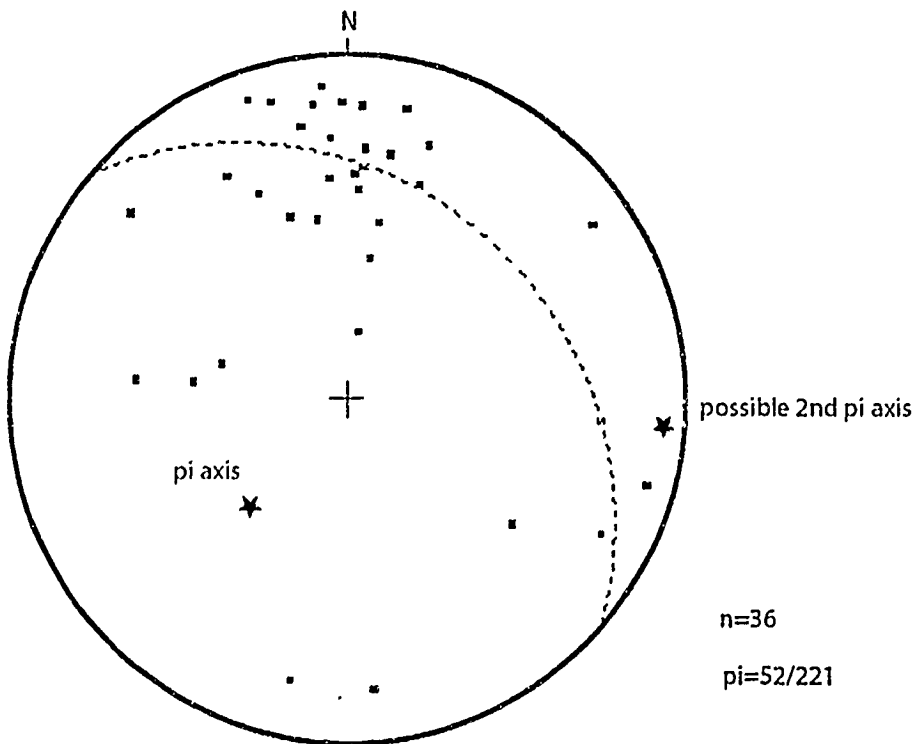


Figure 15. Lower hemisphere projection of poles to beds in the Eastern transect. Projection produced using GEORient 9.2.

south-dipping limb of an anticline with a short north-dipping limb. Folds are markedly asymmetric and are highly non-cylindrical as poles to beds show considerable scatter. It is nearly as possible to draw a pi axis on this stereographic projection at $\sim 05/098^\circ$, which is much more compatible with the other transects (Fig. 15).

Overall, the folds in the different transects record north-northeast-south-southwest shortening.

The plunges of axes statistically calculated for individual transects show significant variability in both magnitude and direction. On the Cle Elum River transect, plunges vary by 17° ; axes plunge 2° to the northwest in the north and 15° to the east-southeast in the south. On the Jolly Mountain transect, the axis plunges 12° to the southeast, which is somewhat consistent with the axis on the Cle Elum River transect.

Intraformational Angular Unconformity

An intraformational angular unconformity is well displayed ~ 2 km from the north end of the Jolly Mountain transect (Fig. 9). The nearest beds measured below the unconformity are oriented $215/06$ northwest and nearest beds measured above are oriented $082/19$ south. Photo interpretation of Figure 9 indicates $>21^\circ$ of angular discordance. Beds above the unconformity were presumably deposited nearly horizontally when those beneath were oriented

~215/21 northwest, and then beds on both sides of the unconformity were tilted 19° to the south. The unconformity indicates that tilting and erosion of at least parts of the Swauk basin occurred before active subsidence and sediment accumulation ceased in the Swauk Formation. It also indicates that measurements or estimates of stratigraphic thickness are minimum values.

Overtured Section

Detailed study of facing indicators, including scour and onlap surfaces and ripples, was used to evaluate facing direction, and facing was determined for 60 stations in the study area. There were 21 overturned bedding measurements on the Koppen Mountain transect (Plate 1). The majority of the stations documented a $\geq 15 \text{ km}^2$ panel of overturned beds that extends the length of the Koppen Mountain transect and represents $>3600 \text{ m}$ of stratigraphic thickness in the central part of the study area. Bedding on the adjacent Jolly Mountain transect, $\geq 4 \text{ km}$ to the west, is not overturned and shows significant variability in strike (Plate 1). Beds $\sim 3.5 \text{ km}$ northeast of the southern end of the Koppen Mountain transect and adjacent to the contact of the Swauk Formation with the Ingalls ophiolite are upright and moderately steeply south- to southeast-dipping (Plate 1).

In order to further investigate the overturned panel and its relationship to domains of upright beds, a 3.8-km-long transect between the Koppen Mountain

and Jolly Mountain transects was completed where the major transects are closest; this transect crosses the Middle Fork of the Teanaway River (Fig. 16 and Plate 1). Bed attitudes from just west of the Middle Fork and to the east average 283/84 north, and the beds are overturned, analogous to the bedding orientations on the Koppen Mountain transect. Bedding farther west of the Middle Fork, however, is upright and averages 015/27 east (Fig. 16 and Plate 1). No transition between the domains of overturned and upright bedding was exposed. The contact or transition must lie within 0.5 km of the transect length in a thickly forested area. The gently dipping, upright beds on the west dip into the contact or transition, and thus it is unlikely that there is an angular unconformity between the different domains. It is interpreted that the domains are separated by a significant, ~north-south-striking fault. It is difficult, however, to trace this inferred fault to the north or south. The contact of the Swauk Formation with the Ingalls ophiolite is faulted near one possible projection of the inferred fault (Plate 1). The inferred fault may connect with the faulted Ingalls-Swauk contact or merge with the map-scale shear zone before reaching the contact. Alternatively, the transition may represent the narrow hinge zone of a fold responsible for overturning the Koppen Mountain strata. Given the high angle between the strikes of beds in the two domains, any such fold is probably highly non-cylindrical. Another alternative is that the transition represents both a fault and a narrow hinge zone (Figs. 17 and 18). In this scenario, the overturned panel is interpreted as the overturned limb of a southwest-vergent syncline with the hinge

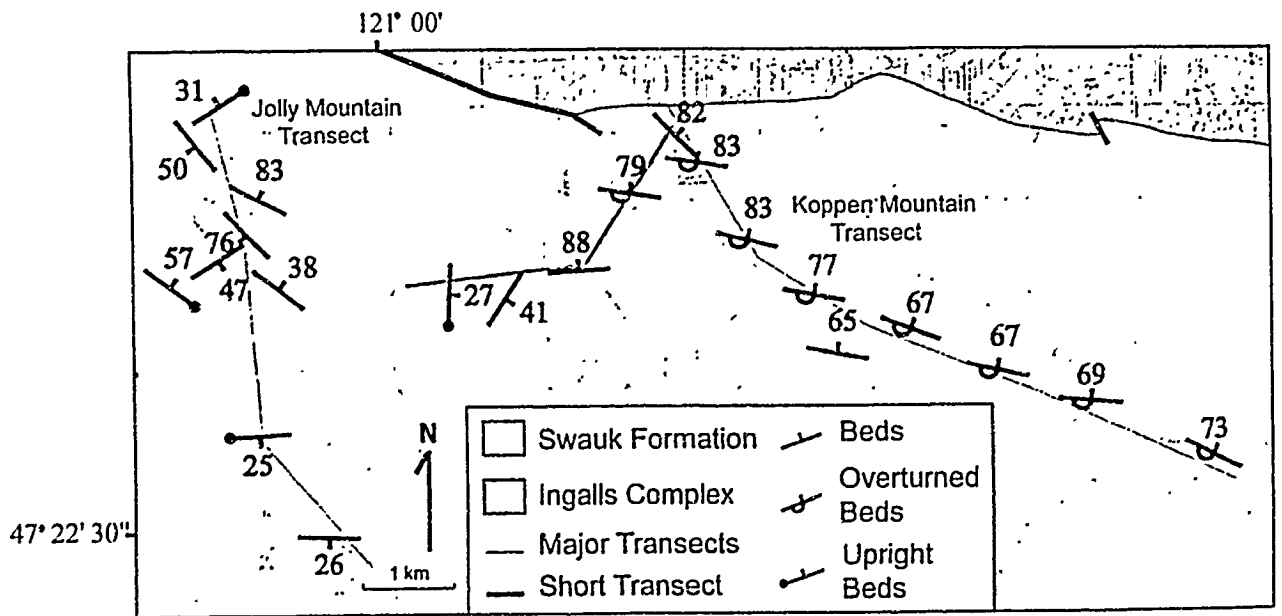


Figure 16. Location of short transect. Representative bedding attitudes from the short transect and the Jolly Mountain and Koppen Mountain transects are shown.

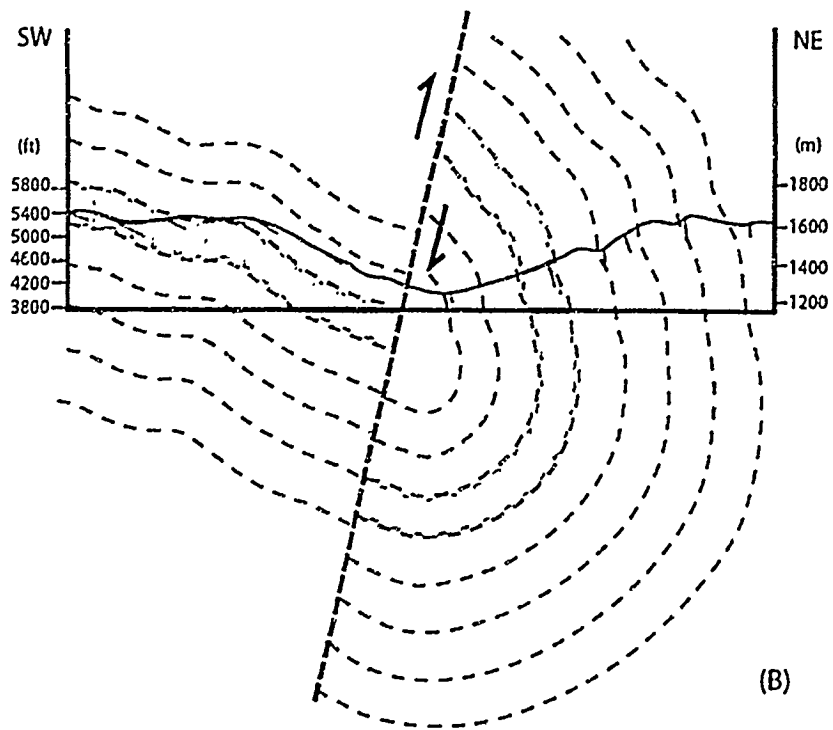
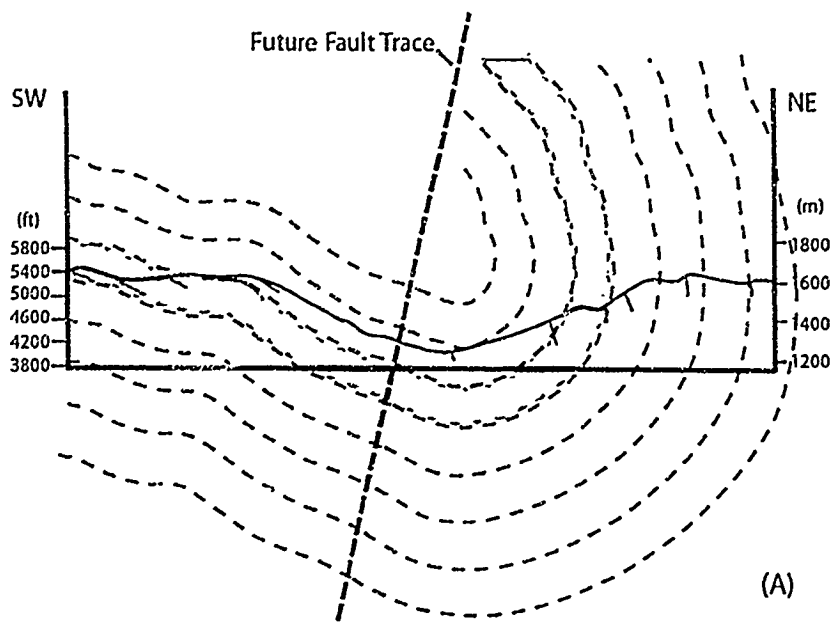


Figure 17. Reverse fault model for overturned strata along Koppen Mountain transect. (A) A reconstruction of unfaulted strata and (B) the strata after reverse faulting. No vertical exaggeration.

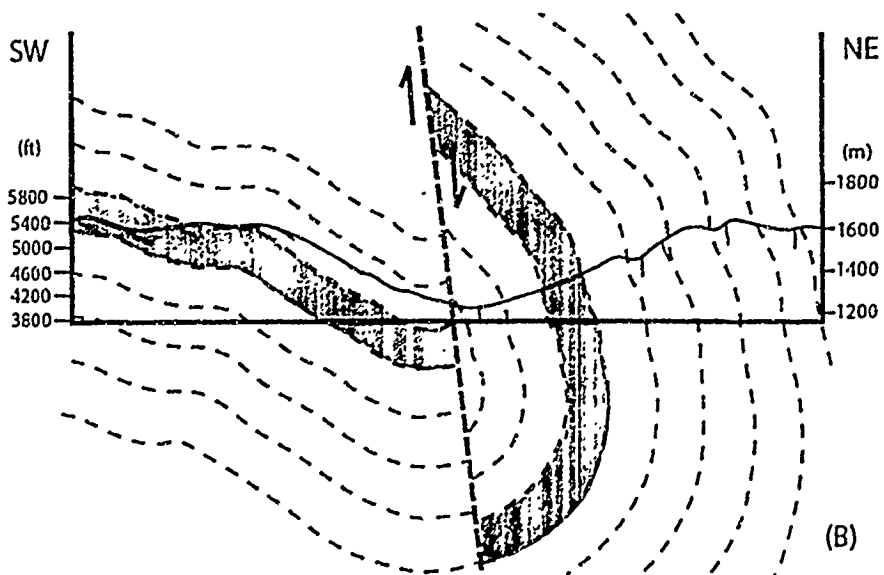
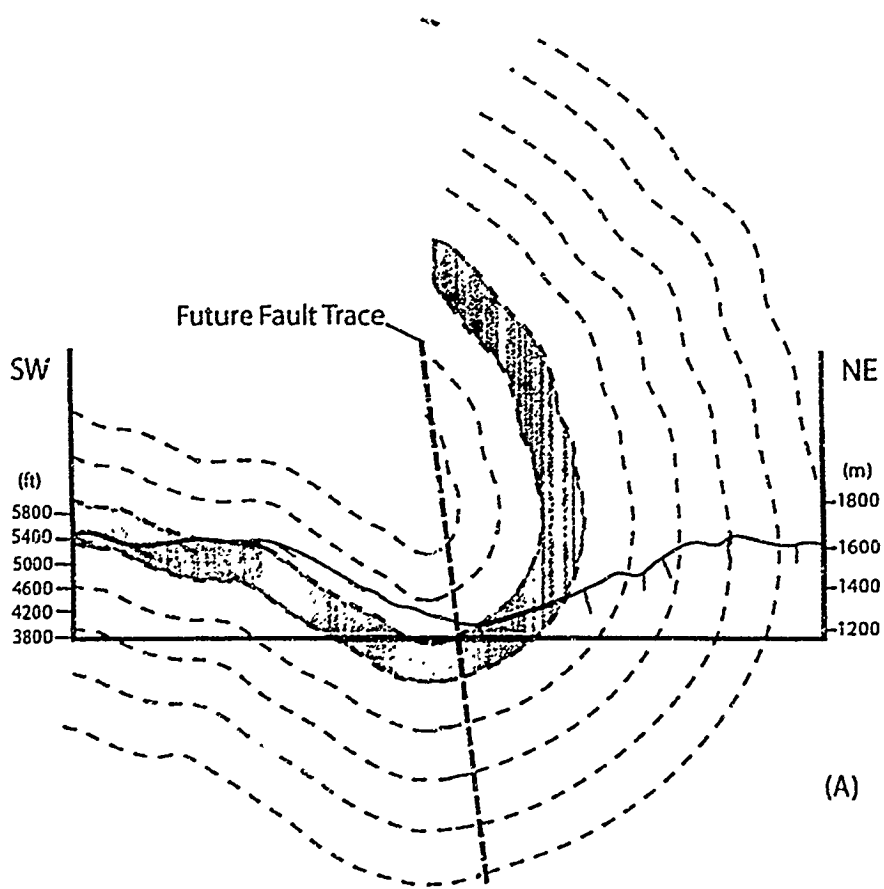


Figure 18. Normal fault model for overturned strata along Koppen Mountain transect. (A) A reconstruction of unfaulted strata and (B) the strata after normal faulting. No vertical exaggeration.

zone cut out by faulting. The inferred syncline would have a northwest or southeast-trending axis, which is consistent with large folds in the field area. The fault necessary to hide the hinge zone could be either a northeast-trending, southeast-side-down normal fault or a northwest-trending, northeast-vergent reverse fault (Figs. 17-19). A reverse fault is more compatible with the shortening recorded by the folding, but the displacement of the fault is in the opposite direction of fold vergence. There is no vergence problem with the normal fault model, but a normal fault would presumably be the product of a later kinematic regime. Finally, the proposed normal fault may actually be an oblique strike-slip fault. Strike-slip along a fault with this orientation would accommodate the differential shortening of strata to the east and west.

Faults

Faults have been mapped within parts of the Swauk basin but have only been briefly described. Ellis (1959), Foster (1960), and Ashleman (1979) mapped many northwest-striking faults cutting the Swauk Formation west of the study area, and Tabor et al. (1982), Johnson (1985), Taylor et al. (1988), and Cheney and Hayman (2009) mapped several north-northeast- and northwest-striking faults east of the study area (Tabor et al., 1982). In the study area, only the inferred faults bounding a shear zone (discussed below) and faulted sections

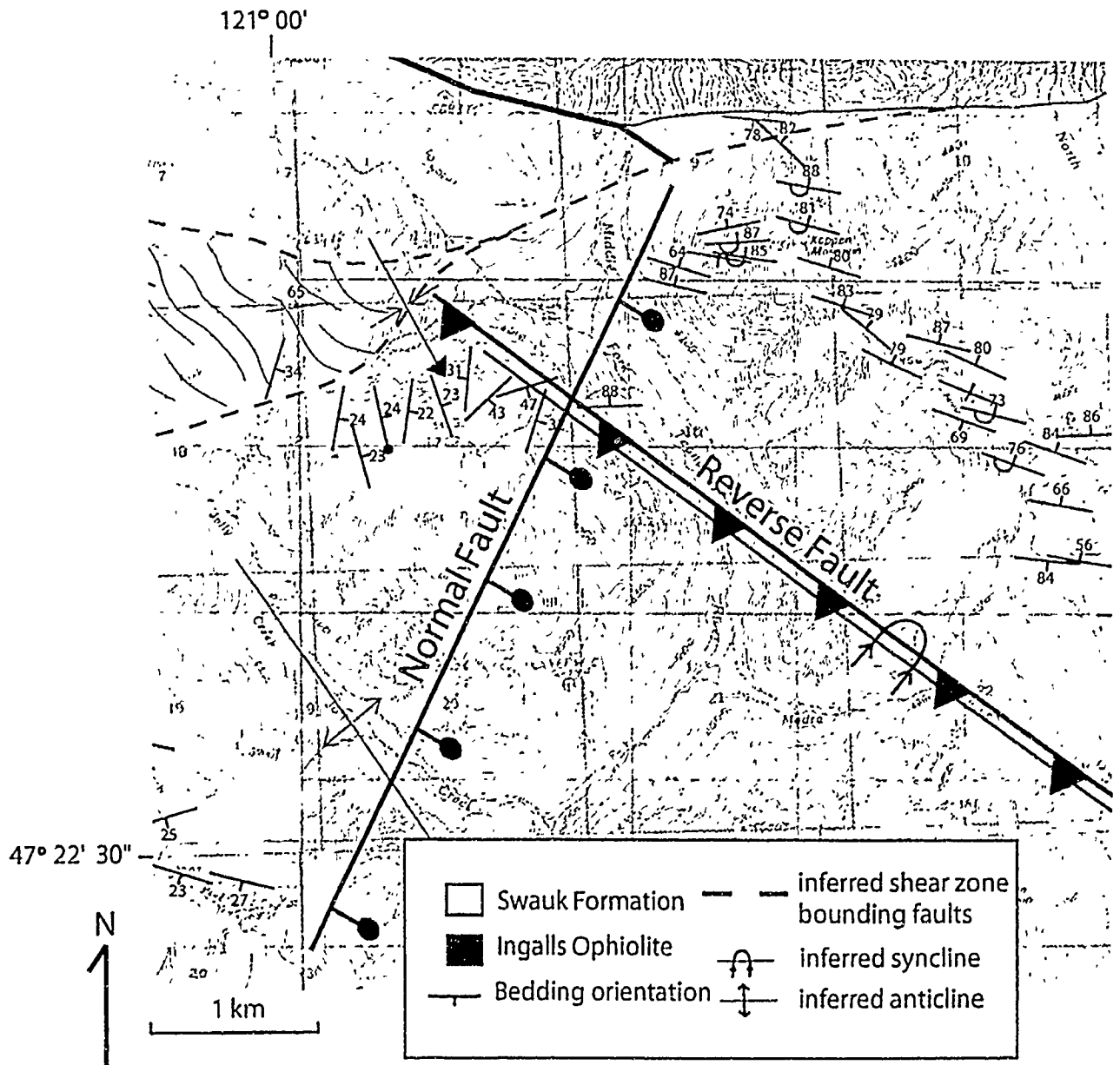


Figure 19. Possible inferred reverse and normal fault trends. The faults explain the transition from the overturned panel on the Koppen Mountain transect and the upright beds on the Jolly Mountain transect.

of the Swauk contact with the Ingalls ophiolite have been mapped by Tabor et al. (1982, 2000), Miller (1985), and MacDonald et al. (2008).

During this study, faults were observed in the field and interpreted from cross-sections. Outcrop-scale faults were recognized by the presence of fault breccias, narrow shear bands, slickensides, and offset beds and dikes. These faults generally strike northwest and dip moderately to steeply (35° - 88°) (Fig. 20 and Plate 1). Faults cut both the Swauk Formation and Teanaway dikes. Of the observed faults, 20% cut Teanaway dikes and no undeformed dikes were observed cutting faults. There are also probably more faulted dikes, but some of the fault planes may have been mistaken for intrusive contacts. Faults were difficult to trace because critical outcrop was commonly missing and because mapping was largely restricted to transects. In cross-section, thrusts and less common, smaller-scale back thrusts are necessary to preserve consistency of bed length at depth in construction of loosely balanced sections (shown in Figures 7 and 8). Reverse faults interpreted from cross-sections are steep (range of 63° - 66°), generally south-dipping, and north-vergent. South-vergent back thrusts are less common (Figs. 7 and 8).

Thin-section study of three fault rocks was done to evaluate kinematic indicators and determine the sense of motion along several of the outcrop-scale faults. Two of the samples (SW-09, SW-146) are from narrow fault zones in Swauk sandstone along the Cle Elum River transect (Fig. 21). A third sample

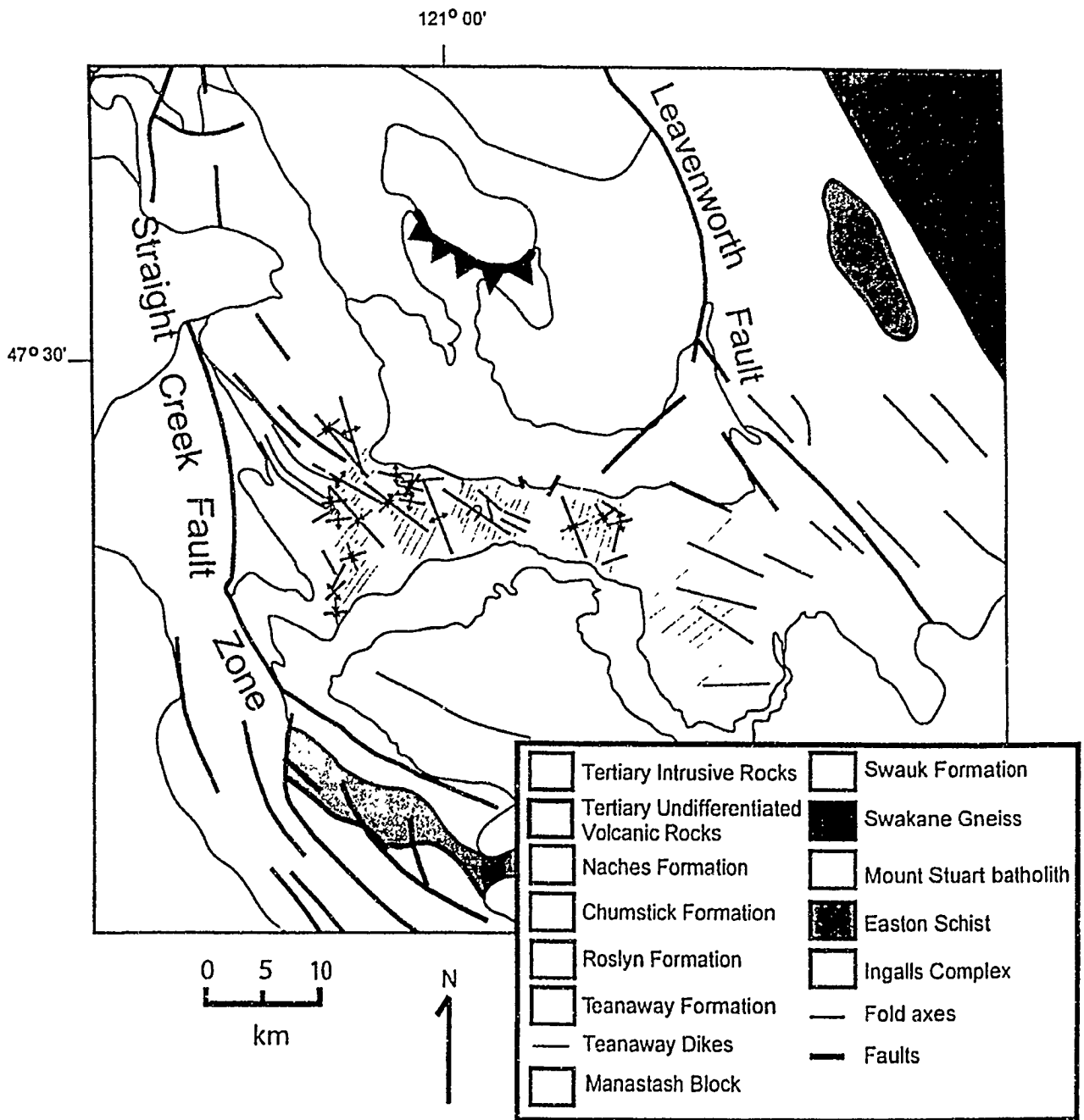


Figure 20. General trends of fold axes, dikes, and faults in and outside the study area. Structures outside the study area are taken from Foster (1951), Ellis (1959), Ashleman (1979), Tabor et al. (1987, 2000), and Mendoza (2008).

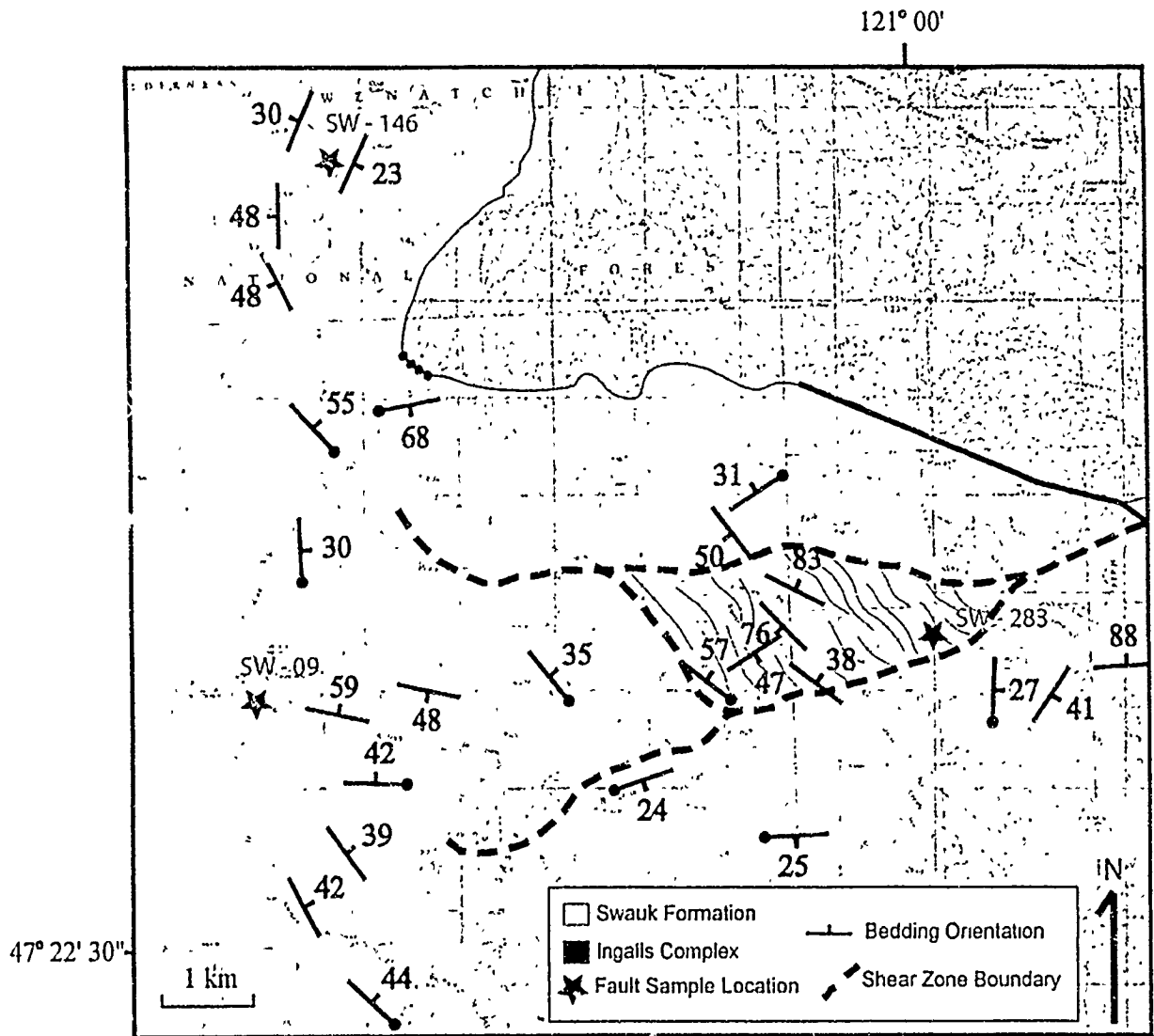


Figure 21. Geologic map of northwest part of the study area. The locations of sampled fault rocks are marked by red stars.

(SW-283) was collected from a fault cutting a Teanaway dike within the shear zone.

Sample SW-09 is a fault breccia along a fault oriented 238/66 northwest, and the sample was collected just east of the Cle Elum River Road and south of Cayuse Campground (Figs. 3 and 21). The sample has slickenside surfaces oriented 232/81 northwest with striae oriented 40/035. In a thin-section oriented nearly perpendicular to the slickenside surfaces, the sample is light-gray, extremely fine-grained, has no distinguishable clasts or sedimentary layers, and is cut by at least two generations of through-going, chaotic, and lighter-gray to white veins of fine-grained, recrystallized quartz and other optically unresolvable material. Veins range in thickness from 0.02 to >1.0 mm with a mean of ~0.5 mm. In some places, veins are ptymatically folded; wavelengths range from 0.2 to >1.0 mm, and interlimb angles from ~121° to ~53°. Offset across microscopic faults indicates dextral-normal motion.

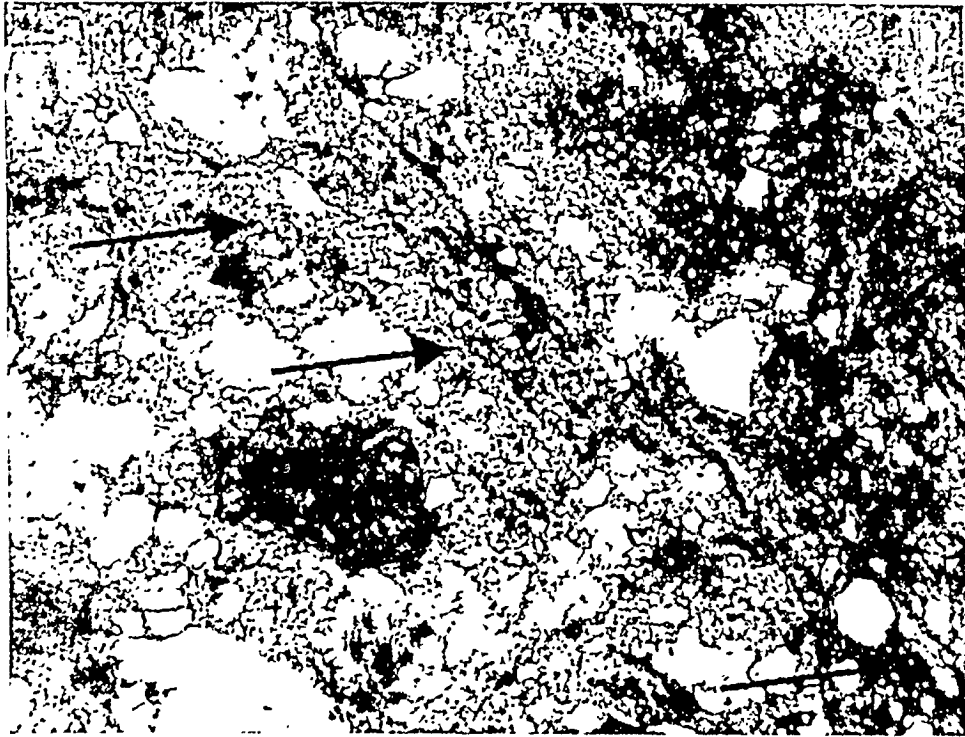
Sample SW-146 is a highly deformed cataclasite with a foliation oriented 124/71 southwest. The sample was collected <1 km from Davis Peak (Fig. 21), at the northern end of the Cle Elum River transect. The sample has slickenside surfaces oriented 106/66 southwest with striae oriented 19/114. Two thin-sections were cut that are perpendicular to foliation, perpendicular to slickenside surfaces, and oblique to striae. In thin-section, bands of pseudotachylyte and/or ultra-cataclasite are abundant and approach ~7 mm in width. The bands consist of tiny (0.05 to < 0.01 mm) angular crystal fragments and larger (~0.2 mm)

rounded quartz grains in a glassy-appearing matrix. The material between the pseudotachylite bands is deformed micaceous, quartz-rich sandstone. The biotite clasts are bent around more competent grains and drawn out into “fish” (Fig. 22). The orientation of striae and offset on Reidel shears and brittle faults, combined with the asymmetry of the mica fish, demonstrate dextral-reverse motion along the fault. In summary, microstructures and kinematic indicators show that both dextral-reverse and dextral-normal faults are present.

Map-scale Shear Zone

A wedge-shaped, map-scale shear zone was mapped at the northern end of the Jolly Mountain transect by Tabor et al. (1982, 2000). The shear zone is oriented 261/65 north at the eastern boundary and is 1.2 km wide at the western end (Fig. 6, Plate 1). The shear zone is well exposed in a cliff on the west side of the Jolly Mountain transect (Fig. 23) and at the western end of the short transect between the Koppen Mountain and Jolly Mountain transects (Fig. 19). From the western edge of this short transect, the map-view contacts of the shear zone were traced. Contacts between the deformed zone and undeformed Swauk sandstone and mudstone to the north and south are not exposed, but the available outcrop suggests that the shear zone has abrupt walls.

Both the Swauk Formation and Teanaway dikes are deformed in the shear zone (Fig. 23). Swauk sandstone in the zone is distinctly bright white with mm-to



1 mm

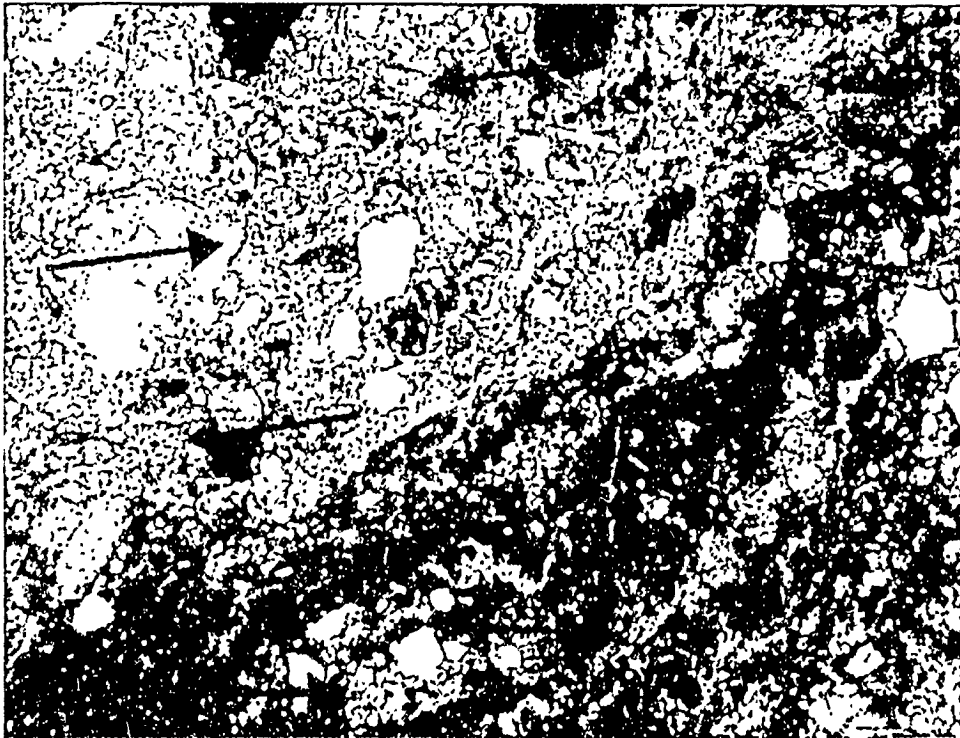


Figure 22. Deformed biotite clasts within pseudotachylyte and/or ultra-cataclasite bands. Both photos of sample S/W-146 are taken within intensely deformed bands of ultra-cataclasite. Possible pseudotachylyte is in the upper right corner of the top image and the lower right corner of the bottom image. Deformed biotite clasts marked by red arrows.

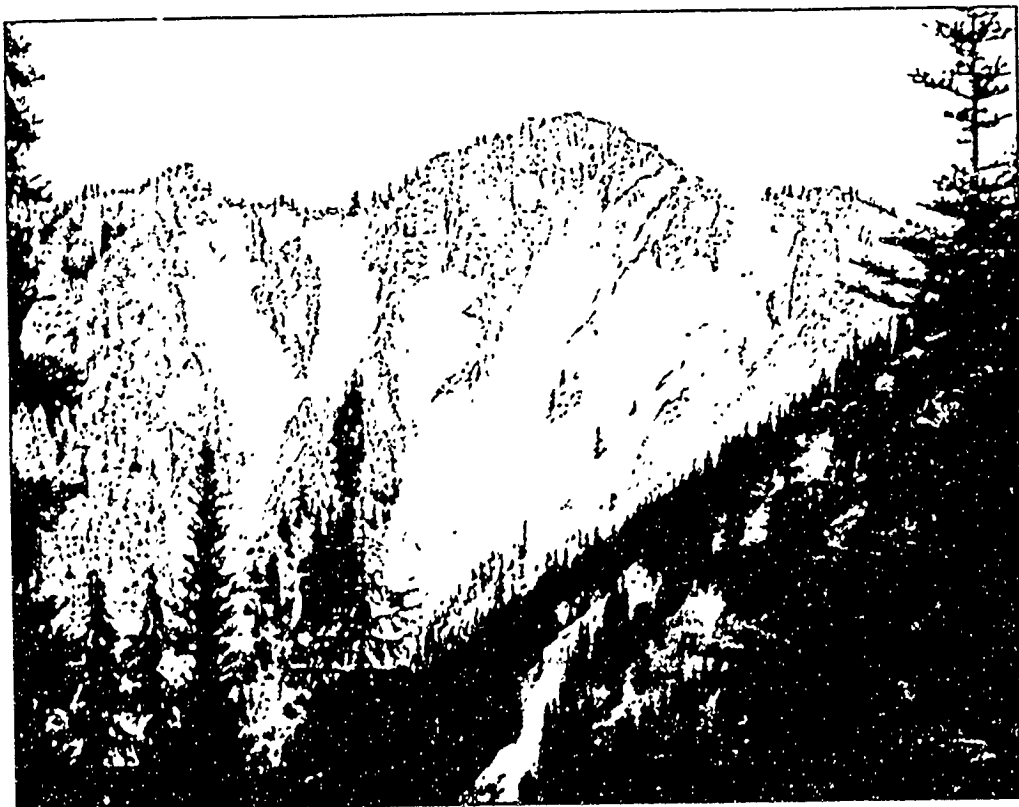
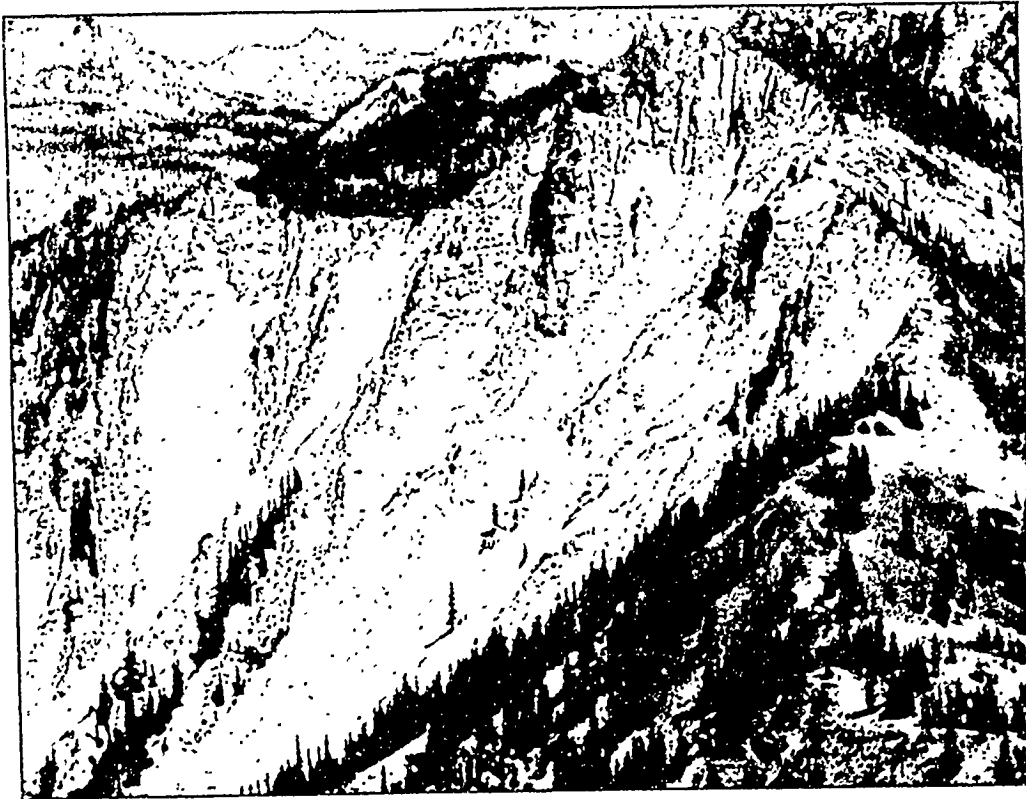


Figure 23. Photographs of the map-scale shear zone. Deformed sandstone and dikes exposed on the west side of the shear zone viewed from the west side of Jolly Mountain (top) and the valley west of the shear zone (bottom).

cm-scale, discontinuous dark layers, which resemble faint remnants of original bedding or, in some places, may be shear bands along which heavy minerals have been concentrated. One such band is oriented 280/88 north. The sandstone has undergone intense grain-size reduction and is now extremely fine grained. It is pervasively fractured and brecciated along a shear band oriented 295/42 northeast. Some shear fractures are striated and separate competent lenses and blocks of deformed sandstone. The dikes are also pervasively fractured and veined. Veins are up to 35 cm wide and chlorite is among the vein-filling minerals.

An ~8 mm wide ductile fault (shear band) cutting an otherwise undeformed dike was found in a thin-section of a dike sample (SW-283) within the shear zone (Fig. 21). The fault is defined by multiple thin (0.1- 1.3 mm wide) bands of semi-opaque zones of extreme grain-size reduction. The bands are bounded by dominantly unaltered dike rock. This fault is oriented 261/65 north and is striated; offset along microscopic brittle faults within the shear band demonstrates dextral-reverse displacement.

Shortening Analysis

Shortening of the Swauk Formation is taken up both by folds and faults. It is impossible to calculate the amount of shortening accommodated by thrust faults in the Swauk basin without recognizing stratigraphic markers. Therefore,

quantification of shortening in this study is limited to the analysis of folds. Because folds in the Swauk Formation are interpreted to have formed by flexural-slip, the original length of stratigraphic layers can be inferred from cross-sections based on the orientations of beds. In order to calculate shortening from folding for a transect, it was first necessary to subtract the total width of Teanaway dikes from the total transect length (Fig. 24). The difference between this adjusted transect length and the “stratigraphic length” was then divided by the stratigraphic length and finally multiplied by 100 to yield a percentage. Shortening calculations were made for the Cle Elum River transect, Jolly Mountain transect, and Eastern transect (Table 2).

The Cle Elum River transect has a weakly constrained total dike thickness and folds accommodate a minimum of 25.6% shortening (Table 2). The Jolly Mountain transect has a well-constrained dike thickness and folds that accommodate a minimum of 28.6% shortening (Table 2). The Eastern transect is ~3.5 km long, has a weakly constrained total dike thickness, and a minimum of 39.3% shortening (Table 2). Shortening increases to the east in the study area.

Teanaway Dikes

Dike Orientation and Thickness

The Teanaway dike swarm extensively intrudes the Swauk Formation and, to a lesser extent, the basement to the formation. The dikes provide evidence for

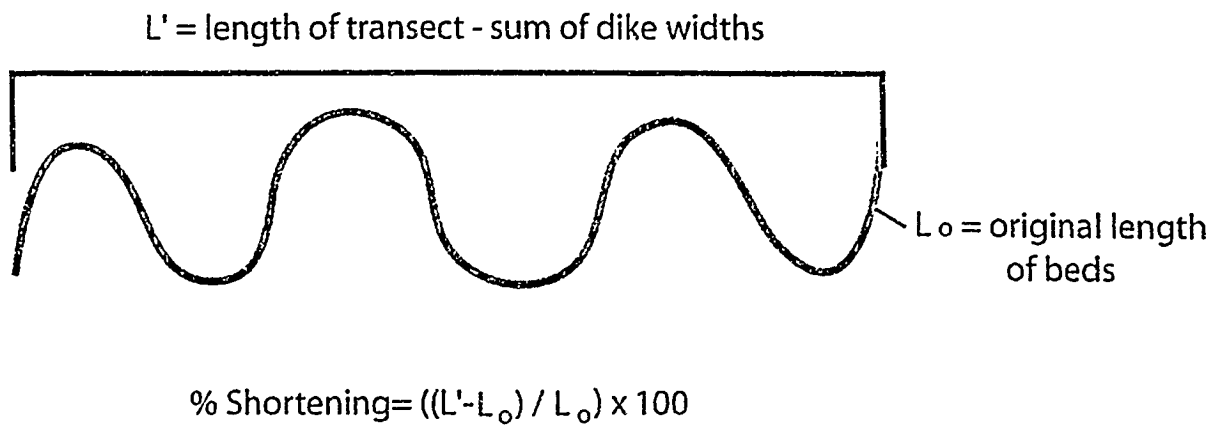


Figure 24. Cartoon illustrating shortening calculations.

Table 2. COMPILATION OF SHORTENING FOR THE CLE ELUM RIVER, JOLLY MOUNTAIN, AND EASTERN TRANSECTS.

Transect	Transect length (km)	Dike thickness (km)	Transect length minus dike thickness (L') km	Length represented by bedding (L_o) km	% shortening	km shortening
Cle Elum R	14.02	0.78	13.24	17.80	-25.62	-4.56
Jolly Mtn	5.69	0.77	4.92	6.89	-28.56	-1.97
Eastern	3.53	0.11	3.42	5.64	-39.33	-2.22

extension after deposition of the Swauk Formation (Foster, 1958). Syn- and post-Teanaway normal faults have not been recognized in the basin, and if present, are unlikely to have contributed much extension. The dikes thus provide the best record of the amount and direction of extension.

To semi-quantitatively analyze extension, dike thicknesses were determined by pacing perpendicular to strike. Dike orientations were measured where contacts were exposed. In many places, only a trend could be measured from the ridge lines along which data were collected. These ridge lines are oblique to the strike of dikes in many places; therefore, pacing was conducted carefully in segments across the crests of the ridges and perpendicular to dike strike. A total of 247 dike orientations were measured in the field area. The most complete dike data set was collected on the Jolly Mountain and Koppen Mountain transects, as these transects run nearly perpendicular to the strike of the majority of dikes in the Teanaway dike swarm.

On the Cle Elum River transect, where 45 dikes were measured, the mean trend ranges from 213° in the north to 203° in the south (Table 3). In the north, 63% of the 16 dikes measured are within 20° of the mean, whereas in the south, only 38% of the 29 dikes are within 20° of the mean. On the Jolly Mountain transect, 48 dike orientations were measured. The mean trend is 204° (Table 3), and 53% of the dike trends are within 20° of the mean. On the Koppen Mountain transect, 95 dike orientations were measured, the mean trend is 203° (Table 3), and 56% of the dike trends are within 20° of the mean. Finally, the mean trend of

Table 3. COMPILATION OF ALL DIKE DATA.

Transect	mean trend (°)	mean dip (°)
N. Cle Elum	213	72
S. Cle Elum	203	64
Entire Cle Elum	206	68
Jolly Mtn.	204	70
Koppen Mtn.	203	64
East	200	67
Combined	203.2	67

the 46 dikes measured on the Eastern transect is 200° (Table 3), and 40% of the dike trends are within 20° of the mean. The mean dike orientation for the study area is $203/67$ northwest. Despite the large variation in dike trends for individual transects, it appears that the mean strike of the dikes from each transect shows a systematic change. From west to east, the mean changes a total of 13° , but mean orientations also change some from north to south along the Cle Elum River transect.

There is large variability in dike dips. The mean dip in the study area is 67° . Dips range from 90° to 21° , and 46% are within 10° of the mean; 12% are less than 50° and 21% are greater than 80° . Dikes generally dip northwest to west-northwest except on the south side of Jolly Mountain on the Jolly Mountain transect, where dikes dip mostly southeast to east-southeast. There does not appear to be any systematic change in dip direction or degree between or along transects. The mean dike dips are as follows: 72° in the north and 64° in the south for the Cle Elum River transect; 70° for the Jolly Mountain transect; 64° for the Koppen Mountain transect; and 67° for the Eastern transect.

Lower-hemisphere stereographic projections of dike orientations along individual transects show that a small fraction of the dikes are nearly perpendicular to the mean. This may be due to inadvertent collection of some orientation data along steps in dikes, sills, or faulted surfaces, all of which have been observed in the study area. These errors may also correlate with some of the gently dipping dike orientations.

Dikes were presumably injected almost vertically (Anderson, 1951). Given the high variability in dips and in order to reduce error produced by data acquisition along sills or steps, the measurements of gently dipping dikes were filtered out and steeply dipping dike data were reanalyzed. Discounting the dikes that dip $<50^\circ$ resulted in decreased scatter in the dike trend data and changed the mean dike trends. The mean for the Cle Elum River transect is consistent from north to south at 216° (Table 4). The mean trend for the Jolly Mountain transect is 208° , for the Koppen Mountain transect it is 201° , and for the Eastern transect it is 197° (Table 4). The new means show a more convincing swing from 216° in the west to 197° in the east (Table 4).

Dike thicknesses range from 13 cm to >80 m. The thickest dikes may be composite and have internal contacts, but were measured as single dikes if no Swauk Formation was preserved between them. Means for the individual transects range from 12 to 20 m. Statistical analysis of mean dike thickness at 500 m increments along transects indicates that no systematic change in thickness occurs across strike for the Jolly Mountain and Koppen Mountain transects, but, on average, dikes are thicker in the southeastern half of each transect (Fig. 25).

Table 4. COMPILATION OF ALL DIKE DATA WITH DIPS >50°.

Transect	# dikes dipping >50°	mean trend (°)	mean dip (°)
N. Cle Elum	13	216	73
S. Cle Elum	20	216	70
Entire Cle Elum	33	216	71
Jolly Mtn.	36	208	72
Koppen Mtn.	86	201	68
East	38	197	70
Combined	193	204	70

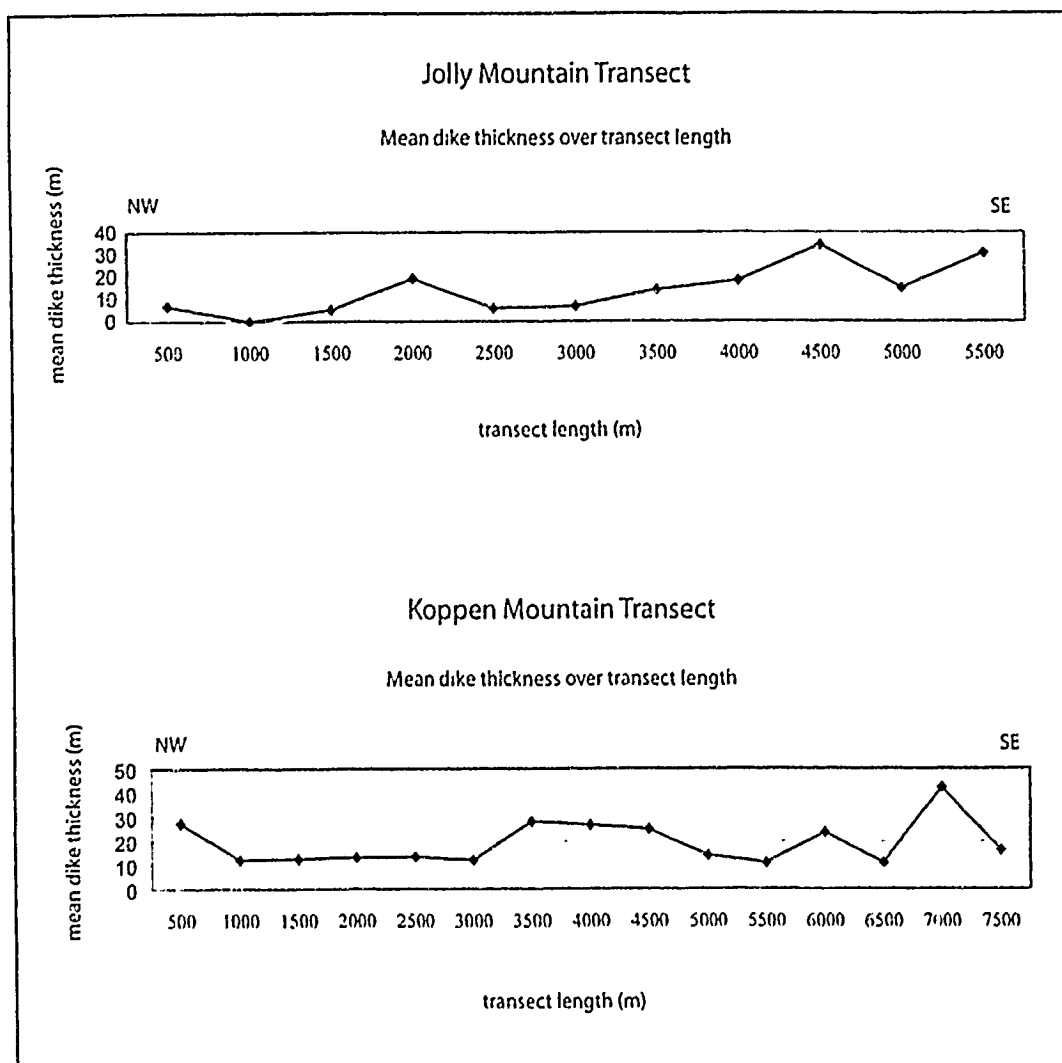


Figure 25. Statistical analysis of dike thicknesses along transects. Mean dike thicknesses plotted every 500 m along the length of the Jolly Mountain and Koppen Mountain transects.

Extension

The Teanaway dikes are interpreted to intrude the Swauk Formation perpendicular to the local extension direction (Foster, 1958). From west to east, mean extension directions vary from 306° - 126° to 287° - 107° and are sub-horizontal. Extension was most closely analyzed for the Jolly Mountain and Koppen Mountain transects.

The Jolly Mountain transect is ~5.7 km long. Thicknesses of 41 dikes were measured with a mean thickness of ~18.7 m and a total thickness of 0.77 km. Teanaway dikes thus accommodate a minimum of ~16% extension along this transect (Table 5, Fig. 26).

Thicknesses of 127 dikes were measured on the ~7.8-km-long Koppen Mountain transect. Dikes along this transect have a mean thickness of ~17.4 m and a total thickness of 2.2 km. Therefore, Teanaway dikes accommodate a minimum of 40% extension along this transect (Table 5, Fig. 26).

Error in extension calculations may arise from three sources. (1) Dikes that dip $<50^{\circ}$ record less horizontal extension. These gently dipping dikes have a total thickness of 2.5 m on the Jolly Mountain transect and 135 m on the Koppen Mountain transect (Table 6). When these values are subtracted from the total dike thicknesses for each transect and extension is recalculated, the maximum error due to gently dipping dikes is $<0.5\%$ for the Jolly Mountain transect and 8.3% for the Koppen Mountain transect (Table 6). (2) Errors arise from the

Table 5. COMPILATION OF EXTENSION DATA FOR THE JOLLY AND KOPPEN MOUNTAIN TRANSECTS.

Transect	Length of Transect (km)	# Dikes	Mean Dike Thickness (m)	Total Thickness of Dikes (km)	% Extension
Jolly Mountain	5.69	41	18.7	0.77	15.6
Koppen Mountain	7.80	127	17.4	2.21	39.6

L' = Length of transect - sum of dike widths



$$\% \text{ Extension} = (\text{sum of dike widths} / L') \times 100$$

Figure 26. Cartoon illustrating extension calculations.

Table 6. CALCULATIONS FOR MAXIMUM ERROR IN EXTENSION DUE TO THE INCLUSION OF DIKES THAT DIP <50°.

Transect	Total Thickness of Dikes (km)	Thickness of Dikes Dipping <50°(m)	Adjusted Total Dike Thickness (km)	Adjusted % Extension	Maximum % Error
Jolly Mountain	5.69	2.5	0.77	15.5	0.45%
Koppen Mountain	7.80	135.0	2.08	36.3	8.30%

inability to collect data on covered parts of the transects (Table 7). When the length of the covered sections of each transect is subtracted from the transect length in the original extension calculations, the % extension increases from 15.6% to 16.7% for the Jolly Mountain transect and from 39.6% to 45.0% for the Koppen Mountain transect. After a 5% allowance for field error, the maximum % error in extension due to cover is 12.3% for the Jolly Mountain transect and 18.6% for the Koppen Mountain transect; however, dikes are commonly the most resistant component along ridges, and it is more likely that poorly exposed portions of the transects represent less resistant Swauk Formation rather than dikes. (3) Errors in measurements may be induced by using paces in an area of rugged topography. These errors would presumably roughly balance out. In summary, considering all of the sources of errors, it is likely that the original extension percentage values of 16% for the Jolly Mountain and 40% for the Koppen Mountain transects are reasonable minima.

Contact Relationships of the Swauk Formation

Contact with the Ingalls Ophiolite

The basal Swauk Formation lies mostly on the Ingalls ophiolite complex (Fig. 2). Relationships along the contact vary from location to location. Generally, the contact is faulted, but it appears to be depositional in some

Table 7. CALCULATIONS FOR MAXIMUM ERROR IN EXTENSION DUE TO COVERED PORTIONS OF TRANSECTS.

Transect	Adjusted Length of Transect (km)	Total Thickness of Dikes (km)	Adjusted % Extension	% Error on Extension	Maximum Error + 5% field error
Jolly Mountain	5.35	0.77	16.7	7.3	12.3%
Koppen Mountain	7.13	2.21	45.0	13.7	18.6%

localities to the east (Plate 1). The basal Swauk Formation is a laterite composed of ironstone. Outcrop of the laterite layer is discontinuous, but the laterite is observed along the Ingalls contact on the Cle Elum River, El Dorado Creek just east of the North Fork of the Teanaway River, and above Bean Creek (Plate 1). These locations are described from west to east.

On the Cle Elum River, the laterite is ~2 m thick. The laterite-Ingalls contact, viewed from across the river, was estimated to have an orientation of 128/65 southwest, and bedding in adjacent Swauk sandstone is oriented 086/68 south (Plate 1). The 32° of discordance in strike between bedding and the contact, and the shear fabric in the adjoining serpentinite imply that the contact is a fault, but little of the Swauk section has been cut out. Near El Dorado Creek, the contact is a fault oriented 285/63 north and is marked by sheared and brecciated serpentinite. There is ~3 m of laterite above the Ingalls contact. Both the laterite and serpentinite are thrust over Swauk sandstones with >3 m offset on an west-vergent thrust oriented 005/35 east. Above the laterite is a thin exposure (~10 m thick) of sedimentary serpentinite. On Bean Creek, the contact between an ~5-m thick section of laterite and serpentinite of the Ingalls Complex is oriented 086/76 south, and although the laterite is sheared, the contact is interpreted as largely depositional.

In locations where the laterite does not crop out, there is also considerable variability in the characteristics of the Ingalls-Swauk contact. Near Koppen Mountain (Plate 1), the contact is oriented 095/78 south, whereas bedding in the

Swauk sandstone above the contact is oriented 310/82 northeast. The 35° of discordance in strikes and the slightly steepened dips of the beds in the Swauk Formation towards the contact indicate that the contact is faulted. On the Eastern transect, the Swauk-Ingalls contact is oriented 065/74 southeast, and just above the contact, bed attitudes are 080/69 southeast (Plate 1). The sandstone above the contact is very fine grained, dark, and veined. It grades to dark, gravel-rich sandstone and then to medium-fine, light sandstone interbedded with dark, silty mudstone. The contact is roughly conformable; however, veining in the Swauk sandstone indicates some shear.

Contact Between the Swauk Formation and Teanaway Formation

The Teanaway Formation unconformably overlies the Swauk Formation (Smith, 1904; Foster, 1958; Tabor et al., 1982). In the study area, the contact was observed in two places; at the southern end of the Cle Elum River transect along Lake Cle Elum and on the southern segment of the Koppen Mountain transect (Fig. 6). On the Cle Elum River transect, the contact is covered, but is identified by the southernmost outcrop of Swauk sandstone. On the Koppen Mountain transect, the contact is also covered. Adjacent to the contact, the Swauk Formation consists of massive, medium-coarse- to medium-fine-grained, light sandstone with upright large trough cross-beds, and beds are oriented between 101/46 south and 072/56 southeast. Bedding in the Teanaway

Formation, as defined by the contact between an altered volcanic breccia and tuff, is oriented 221/31 northwest (Fig. 27). Beds in the younger (~47 Ma; Tabor et al., 1984) Teanaway Formation dip gently northwest into and are discordant to the mapped contact (e.g., Tabor et. al., 1982), which indicates that the contact at this locality is faulted.

DISCUSSION

The following discussion is divided into four parts. Shortening of the Swauk basin as determined from bed orientations and folds is discussed first. Then, faults and the Ingalls-Swauk contact are addressed followed by a discussion of the extension of the Swauk basin as represented by the Teanaway dike swarm. Finally, regional implications are discussed.

Bed and Fold Orientations

Previously mapped fold axial traces at the 1:100,000 scale in the study area trend southeast with as much as 25° of curvature (Foster, 1958; Tabor et al., 1982, 2000). This study involved mapping bed orientations at a 1:24,000 scale, which revealed that hinge lines show more variability than was previously recognized and vary significantly from transect to transect and within each transect. Analysis of data plotted on stereographic projections and interpretation

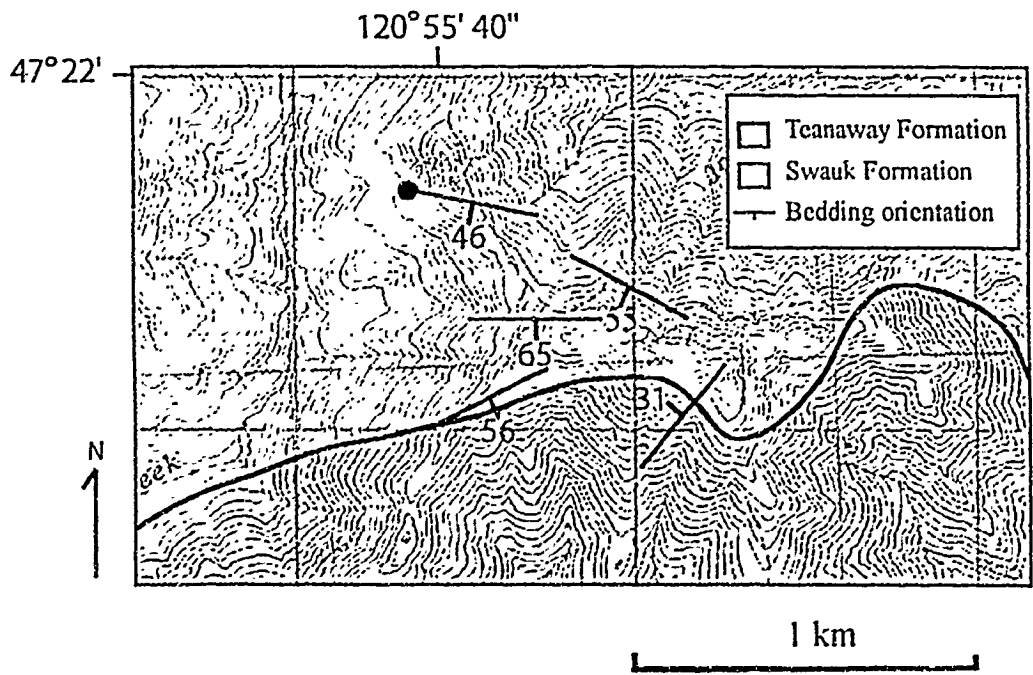


Figure 27. Geologic map of part of the Swauk-Teanaway contact. The map emphasizes bedding and the contact between the Teanaway Formation and Swauk Formation south of Johnson Creek (contact modified from Tabor et al., 2000).

of dip reversals from bedding orientations show that fold axial trends range from northwest-southeast to nearly east-west along the Cle Elum River transect, on the western edge of the study area, to east-northeast along the Eastern transect. Plunges are gentle, and plunge directions are inconsistent. Because of the significantly different trends, stereonet analysis and calculation of P_1 axes is not simple or necessarily diagnostic in analyzing the style of folding and orientation of folds; however, stereonet analysis of P_1 axes indicates that axial planes strike northwest for the north half of the Cle Elum River transect, east-southeast for the south half of this transect, and east-southeast for the Jolly Mountain transect.

The axial curvature in previously mapped folds may represent two separate generations of folding. Poly-phased folding may account, at least in part, for the high variability in trends of axes throughout the study area.

Interpretation of cross-sections and bed orientations supports two generations of folds in the Swauk Formation that pre-date intrusion of the Teanaway dikes (Figs. 7 and 8, Plate 1). Smaller, east-northeast-trending folds appear to be overprinted by larger northwest-trending folds as axial planes of the east-northeast-trending folds are tilted from upright and folded by the northwest-trending ones (Figs. 7 and 8, and Plate 1). The east-northeast-trending folds are more prevalent to the east in the study area.

Volcanic flows of the Teanaway Formation and younger nonmarine sedimentary rocks of the Roslyn Formation and Chumstick Formation have also been folded. These younger formations are deformed into an open syncline that

has a gently southeast-plunging hinge line and a wavelength of >25 km (Fig. 20). Therefore, the Swauk Formation probably underwent three phases of shortening.

The axial trends of the dominant northwest-trending folds (second generation) broadly fit with a classic wrench model for dextral slip along the Straight Creek fault (Ashleman, 1979; Vance and Miller, 1979, 1981; Johnson, 1985; Taylor et al., 1988). The wrench model predicts that folds and thrust faults are oriented at $\sim 45^\circ$ to the strike of the master fault. In a modification to the wrench model, where transpression is dominant, the angle decreases to $\sim 25^\circ \pm 10^\circ$ (Fig. 28) (e.g., Sanderson and Marchini, 1984). Strain and stress partitioning models predict an even lower angle between strike-slip faults and fold axial traces where two sets of structures are developed to accommodate pure and simple shear components, respectively (Zoback et al., 1987; Robin and Cruden, 1994; Tikoff and Teyssier, 1994). The Straight Creek fault trends $\sim 350^\circ$ - 170° along the western boundary of the majority of the Swauk Formation. Axes of large folds in the formation are generally northwest-trending, at a moderate angle (24° - 60°) to the trend of the Straight Creek fault. Axial traces to the west of the study area approach the strike of the Straight Creek fault more closely (Fig. 20) and folds become tighter and are more widespread with proximity to the fault (Foster, 1958; Ellis, 1959; Ashleman, 1979). The acute angle between the Straight Creek fault and axial traces of both the large folds in the study area and those that have been mapped to the west support a wrench model for already well documented right-lateral motion along the Straight Creek fault (Fig. 20).

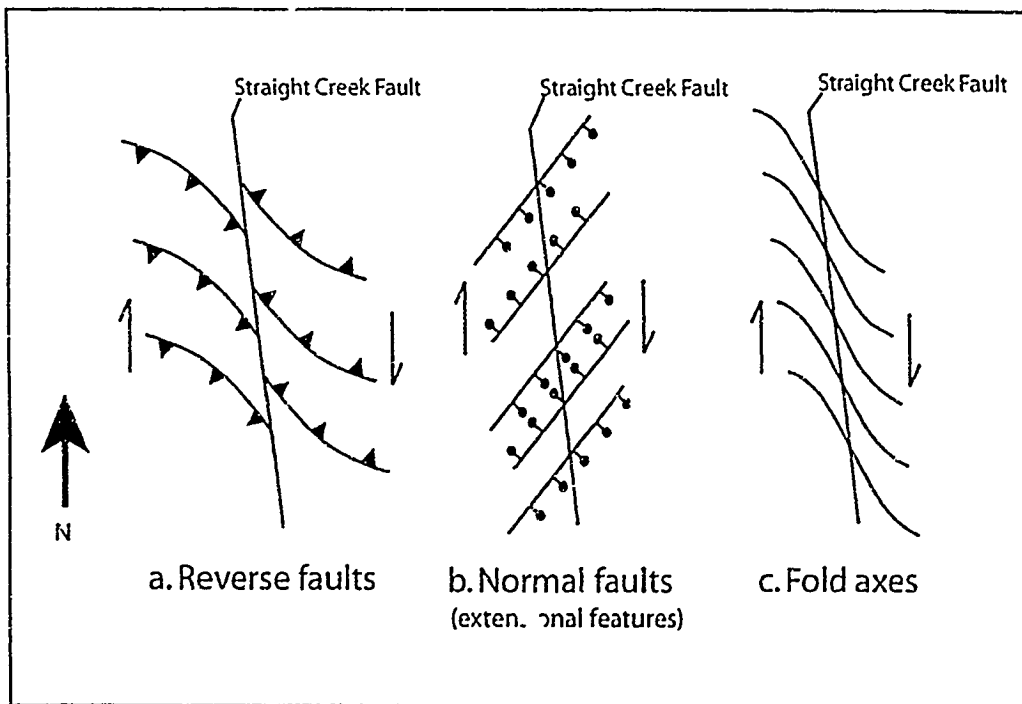


Figure 28. Structures in a typical wrench model. Orientations of faults, folds, and extensional features have been rotated for a wrench tectonic model oriented similar to the Straight Creek fault (modified from Twiss and Moores, 1992).

However, a wrench model can not readily explain why northwest-trending folds are developed >25 km from the Straight Creek fault.

Dextral motion on the Straight Creek fault is thought to have initiated after mostly vertical displacement during accumulation of the Swauk Formation (Tabor et al., 1984). The smaller east-northeast-trending folds in the study area may have formed before initiation of dextral motion on the fault. In one scenario, both the east-northeast-trending and northwest-trending folds resulted from regional shortening that predated strike-slip. These folds may have been rotated and tightened as a result of later dextral displacement on the Straight Creek fault.

Documented motion in the Leavenworth fault zone is largely vertical and was followed by strike-slip (Taylor et al., 1988; Evans, 1994; Cheney and Hayman, 2009). Northwest-trending folds in and adjacent to the Leavenworth fault zone may be associated with reverse motion in the zone (Cheney and Hayman, 2009). I favor strike-slip because fold axial traces west of the Leavenworth fault swing toward near-parallelism with the fault zone as the structure is approached (Fig. 20). Further evidence for dextral motion on the Leavenworth fault includes transpression at left-stepping bends, formation of small-scale pull-apart basins, and horsetail splays in the Chumstick basin (Evans, 1994).

The Swauk Formation probably correlates with the Chuckanut Formation, which has been truncated and dextrally displaced to the north-northwest by the Straight Creek fault (e.g., Frizzell, 1979; Johnson, 1984; Taylor et al., 1988).

Folds in the Chuckanut Formation are north-northwest- to west-northwest-, and locally west-trending (Johnson, 1985; Dragovich et al., 2002). If the east-northeast-trending folds in the Swauk Formation were formed by regional shortening before initiation of strike-slip along the Straight Creek fault, and the two formations are correlative, then the Chuckanut Formation should have similarly oriented folds; however, few folds of this orientation have been documented in the Chuckanut Formation.

The intensification of deformation towards the center of the Swauk Formation (eastern part of the study area) and to the north in individual transects is an important structural observation. Minimum percent shortening increases from 25.6% for the Cle Elum River transect in the west, to 28.6% for the Jolly Mountain transect, to 39.3% for the Eastern transect. The eastern lobe of the Swauk basin is not part of the study, but inspection of cross-sections and bedding dips from published maps suggests that shortening decreases significantly with proximity to the Leavenworth fault zone. This variation in shortening may partially account for the overall outcrop pattern of the Swauk Formation with a narrow, highly shortened central zone and broad lobes to the west and east.

Folding intensifies towards the basal contact with the Ingalls ophiolitic complex in the north and dips of beds shallow to the south toward the upper contact with the Teanaway Formation. The dominantly ultramafic rocks of the ophiolite and the mainly tonalitic Mount Stuart batholith are much stronger than

the clastic rocks of the Swauk Formation. Thus, the basement rocks probably acted as a strong buttress, against which the relatively weak Swauk rocks were shortened (e.g., Tabor et al., 1984).

Another potential explanation for the weaker folding and shallower dips to the south is that shortening began during sedimentation. If this was the case, there should be many small intraformational unconformities. One angular unconformity was observed on the Jolly Mountain transect, as described above, but this unconformity is relatively local. Other unconformities may exist, and be unrecognized due to limited outcrop, and/or only small angular discordance, but it seems unlikely that intraformational unconformities are widespread.

Faults

Observed faults and fault zones are scattered throughout the study area (Plate 1). Map-scale faults do not cut the late Eocene Roslyn Formation, and only a few mappable faults, mostly west of Lake Cle Elum, cut the Teanaway Formation (Tabor et al., 2000, 1982). Teanaway dikes in the study area are sheared and faulted in some cases, and 20% of the observed faults in the area cut dikes. Four hypotheses are presented below to explain these structural relationships. (1) It is likely that much faulting of the Swauk Formation largely predates deposition of the Teanaway Formation. (2) More faults than are known involve the Teanaway Formation adjacent to the study area, but are either too

small to map at 1:100,000 or are difficult to recognize without dikes or other markers. (3) Shearing was focused toward the Mount Stuart buttress, leaving the flows of the Teanaway Formation less faulted than the dikes. (4) Some dikes may be slightly older than many flows of the Teanaway Formation and faulting of the dikes occurred shortly after dike solidification and before accumulation of the flows.

The overturned panel that encompasses the entire Koppen Mountain transect (Plate 1) is interpreted as a >3.6-km-thick overturned limb of a southwest-vergent syncline with the hinge zone cut out by faulting. The hinge zone is probably obscured by faulting. A hypothetical reverse fault (Fig. 17) would extend south of the Koppen Mountain transect, beneath the Teanaway Formation and northward into the eastern boundary of the map-scale shear zone (Fig. 19). The orientation and motion of this reverse fault are consistent with shortening that produced the syncline, but the vergence is opposite that of the fold. The fault probably has ~900 m of offset in order to completely remove the hinge zone (Figs. 17), and it is unlikely that a fault of such magnitude would die out before reaching the Ingalls-Swauk contact. There is no evidence of offset of contacts or other structures to support a reverse fault. Therefore this model is not favored.

More likely, the structural relationship results from either a normal fault (Fig. 18) that formed due to extension after shortening or a strike-slip fault that accommodated differential shortening. This normal or strike-slip fault would

strike northeast and extend south of the Jolly Mountain transect and north into the Ingalls contact near Koppen Mountain (Fig. 19). The Ingalls-Swauk contact is defined by a fault that curves into the inferred boundary of the map-scale shear zone approximately where the inferred normal or strike-slip fault extends (Plate 1). This inferred fault probably connects with the faulted Ingalls-Swauk contact or possibly merges into, or is truncated by, the map-scale shear zone before it reaches the contact. The lack of offset of the Swauk-Teaway contact implies that the fault predates accumulation of the Teaway Formation.

Nature of Contact between Swauk Formation and Ingalls Ophiolite

The contact between the Ingalls ophiolitic complex and Swauk Formation varies along strike. The ophiolite consists of sheared serpentinite wherever the contact is observed. Some shear in the ophiolite as a whole is Jurassic in age (Miller, 1985), and thus, it is difficult to determine the extent of Eocene versus older shearing adjacent to the contact. The contact appears depositional in some places in the eastern half of the study area.

The competence of the Ingalls ophiolite and Mount Stuart batholith relative to the layered sedimentary rocks appears to influence the intensity of deformation in the Swauk basin. It is thus reasonable to expect that the contact would be faulted. In areas where the contact appears depositional, shear may be parallel to the contact and difficult to recognize. Strain may also be

partitioned into the weaker sheared serpentinite, leaving the Swauk Formation locally undisturbed. Alternatively, the observed faulted segments of the contact may represent localized shear along an otherwise largely preserved unconformity.

Extension

Teanaway Dikes

The Teanaway dikes record post-shortening extension in the Swauk basin. The dikes are related to the Teanaway Formation, and presumably have a similar origin due to partial melting of the mantle (Tepper et al., 2008). This melting may have been caused by subduction of the Kula-Farallon ridge at ~50 Ma at the latitude of central and northern Washington (e.g., Thorkelson, 1995; Dostal et al., 2003; Breitspecher et al., 2004; Madsen et al., 2006).

The Teanaway dikes show a small, but systematic change in trend and extension direction from the western to eastern parts of the study area (Table 3). After filtering out gently dipping dikes, trends change by 19° from 216° along the Cle Elum River transect to 197° along the Eastern transect (Table 4).

In a wrench model for the Straight Creek fault, extensional features are oriented ~45° to the dextral strike-slip fault and are perpendicular to northwest-trending fold axes. The Teanaway dikes broadly fit this model (Fig. 20), as the Straight Creek fault west of the study area trends 350°-170° and the angle

between the fault and mean dike trend is 46° along the Cle Elum River transect and 27° along the Eastern transect. Arguing against this model, however, dikes intrude the entire Swauk basin, up to ~60 km east of the Straight Creek fault, with sub-parallel orientations (Foster, 1958; Clayton, 1973; Tabor et al., 1982, 2000; Mendoza, 2008). It is thus probable that the dikes were controlled by a regional transtensional regime. Dike orientations more closely approximate a wrench model with proximity to the Straight Creek fault and motion along the fault may have modified the local strain field.

Minimum extension magnitudes associated with intrusion of the Teanaway dike swarm were calculated as ~16% for the Jolly Mountain transect and ~40% for the Koppen Mountain transect (Table 5). Minimum extension magnitudes for part of the Swauk basin east of the study area are ~10.5% (Mendoza, 2008). Increased extension in the center of the basin, far from the Straight Creek fault, further argues against wrench faulting as the major control during dike injection.

An important issue for the timing of folding of the Swauk Formation is the relationship of folds to the Teanaway dikes. The mean dip of dikes observed in the field area is 67° to the northwest, and thus dikes are tilted somewhat from their inferred vertical orientation during intrusion. Dikes are not folded on the outcrop scale, and dike orientations do not define map-scale folds. The dikes almost certainly post-date the first-generation folds, but the relative timing of the dikes and the second-generation folds is less clear. Hinge lines of the gently plunging second-generation folds in the Swauk Formation are roughly

perpendicular to the dikes, and dike orientations would not change significantly due to folding about axes with this orientation. The dip direction of the dikes would change with changing plunge direction, but this relationship is not observed, as dikes generally dip northwest to west-northwest.

In summary, the Teanaway dikes were intruded in a transtensional regime that was locally modified by wrench faulting, minimum extension increases toward the center of the basin, and the dikes post-date the first-generation folds and show little evidence of being folded by the second-generation folds.

Analysis of Mean Dike Thicknesses along Transects

A study of mafic dike swarms associated with the Mid-Atlantic spreading center in Greenland and Iceland has shown that systematic changes in dike thickness with distance from the source can provide information about source geometry and depth (Klausen, 2006). Dikes were found to decrease in thickness and increase in number towards the magmatic source (Klausen, 2006). This relationship was evaluated for the Teanaway dike swarm in the study area.

The Teanaway dikes have been interpreted as a feeder system for the Teanaway Formation (Foster, 1959; Tabor et al., 1982) and a shield volcano, ~6 km west-southwest of the Cle Elum River transect. The shield volcano is also a source of the Teanaway flows according to Clayton (1973). Thus, one

hypothesis is that the main magmatic source for the dike swarm is southwest of the study area.

Analysis of thicknesses of Teanaway dikes along the Jolly Mountain and Koppen Mountain transects shows that dikes are generally thicker in the southeastern half of the transects (Fig. 25). Mean dike thicknesses from each transect increase to the west, towards the shield volcano, from ~14 m east of the study area (Mendoza, 2008), to ~17 m on the Koppen Mountain transect, to ~19 m on the Jolly Mountain transect. Therefore, the Teanaway dike swarm does not fit the model of decreasing dike thickness towards the potential magmatic source; i.e. the shield volcano west-southwest of the study area. Further arguments against the Teanaway dikes as feeders related to the inferred volcano include the fact that the dikes do not show a classic radiating pattern with respect to the volcano, and the dikes extend >50 km east of the inferred volcano.

Klausen (2006) also proposed that thick dikes result from injection through thick, cool crust, and thin dikes often inject, after the thick dikes, once the crust has thinned and the magma source is closer to the surface. The Teanaway dikes are thick with very few cm-scale dikelets. If Klausen's (2006) hypothesis is correct, then the magma source for the Teanaway dikes is relatively deep and dikes were injected into thick, cool crust. Extension and distribution of the dikes are likely related to the opening of a slab window or some other perturbation of the mantle.

Extension and Eocene Dikes Elsewhere in the North and Central Cascades

Mafic to silicic Eocene dikes also intrude parts of the Cascades core north of the Swauk basin and metamorphic core complexes to the east. Orientations of these dikes were used to analyze Eocene extension in the central and North Cascades. Dike data below are from individual dikes associated with plutons and dike swarms.

Dike orientations (Fig. 29) are discussed from south to north. Dikes associated with the ~46 Ma Duncan Hill pluton have a trend of roughly 035° (Tabor et al., 1987), and those related to the southern part of the ~48 Ma Cooper Mountain batholith have a mean trend of 005° (Raviola, 1988). Two sets of poorly dated dikes intrude 76 to 48 Ma orthogneisses in parts of the southern and central Skagit Gneiss Complex (Fig. 29) (Michels, 2008; Shea, 2008). The southern dikes have a mean trend of 032°, whereas the northern dikes have a mean trend of 092° (Michels, 2008; R.B. Miller, unpublished data; Shea, 2008).

The mean extension direction of the Duncan Hill, southern Skagit, and Cooper Mountain dikes have orientations that overlap those of the Teanaway dikes; however, the dikes that intrude the central part of the Skagit Gneiss Complex record an extension direction of ~002°, which is anomalous with respect to all of the other dike swarms in the Cascades. Dike extension directions from across the North and Central Cascades thus do not have a simple pattern or systematic variation. Nevertheless, broadly northwest-southeast, arc-parallel to

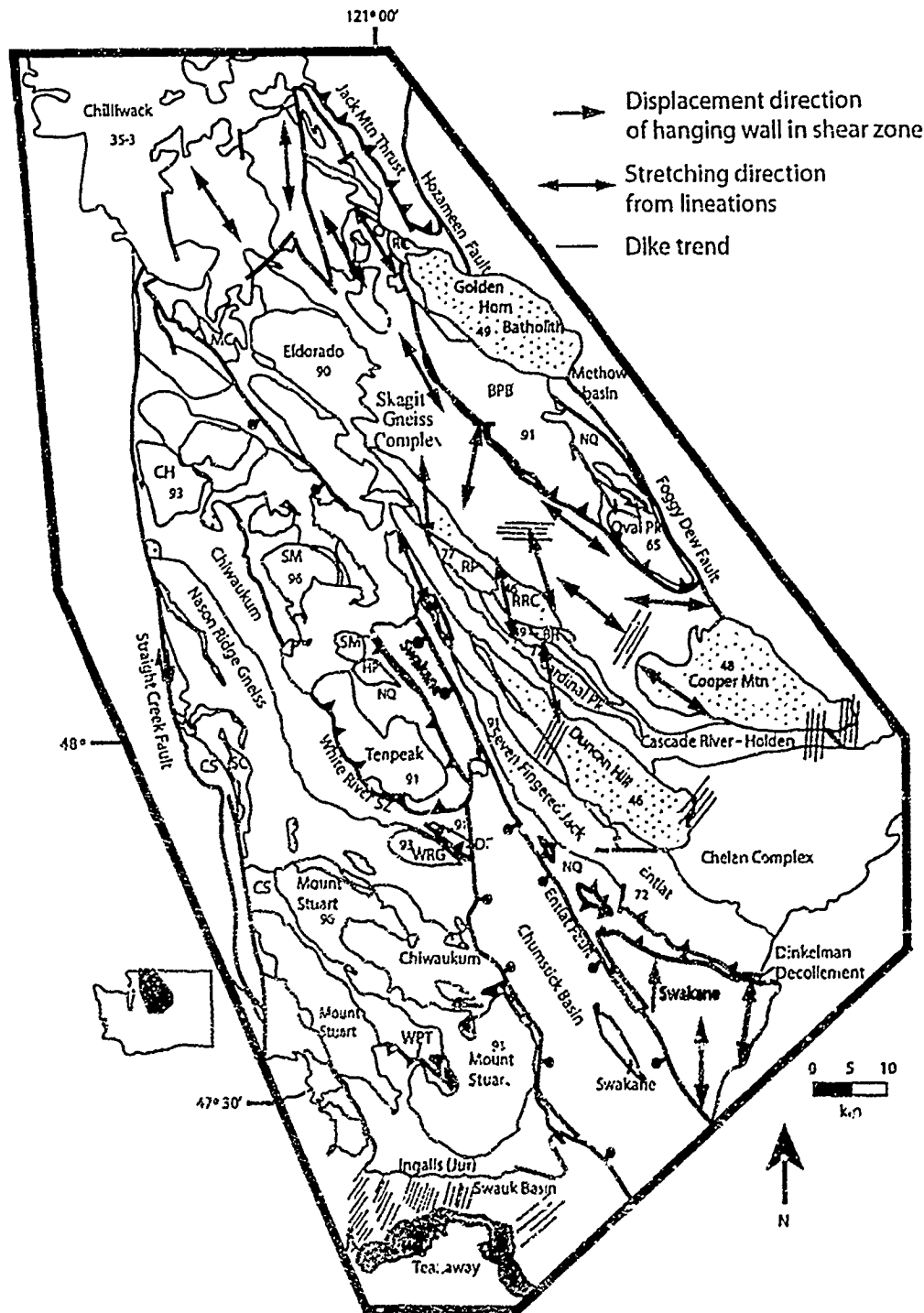


Figure 29. A portion of the North Cascades crystalline core and adjacent Chumstick and Swauk basins. Eocene plutons are in orange and ages are in Ma. Red lines represent middle Eocene dike trends. BPB -- Black Peak batholith; BR -- Bearcat Ridge Orthogneiss; CH -- Chavai pluton; CS -- Chiwaukum Schist; DF -- Dirtyface pluton; MC -- Marble Creek pluton; NQ -- Napeequa Complex; RLF -- Ross Lake fault, RP -- Riddle Peaks pluton; RRC -- Railroad Creek pluton; SC -- Sloan Creek pluton; SM -- Sulphur Mountain pluton; WPT -- Windy Pass thrust; WRG -- Wenatchee Ridge Gneiss;

arc-oblique extension is recorded by the dikes from the Cascades core, adjacent rocks, and the Teanaway dike swarm.

The variability in extension direction implies complex spatial changes in the regional strain field. Alternatively, the dikes are not well dated and they may have slightly different ages; therefore, they may be sufficiently different in age to reflect different orientations of a rapidly changing regional strain field (Doran et al., 2007).

To the east of the Cascades core, Eocene dikes adjacent to Eocene core complexes record east-west extension, roughly perpendicular to the long axes of the complexes. For example, Eocene dikes adjacent to the Republic graben, ~175 km northeast of the study area, record orogen-perpendicular, east-west extension (McCarley Holder, 1990). This contrasts with arc-parallel to arc-oblique, northwest-southeast extension recorded in the Cascades core to the west. The effects of strike-slip along the plate boundary may be responsible for the disparity.

Regional Implications

Determination of the relationship between shallow-crustal deformation of the Swauk Formation and ductile deformation of structurally deeper rocks on the northeastern part of the Cascades core is one of the major goals of this study. In particular, the comparison of this deformation enables evaluation of the degree of

coupling between different crustal levels in the central and North Cascades during the Eocene.

Ductile structures of Eocene age in the deeper rocks include major ductile shear zones, like the Dinkelman decollement (Fig. 29), which records top-to-the-north shear (Paterson et al., 2004). In the Skagit Gneiss Complex and intruding plutons, Eocene stretching lineations are broadly northwest-southeast-trending, gently plunging, and arc-parallel, except in the central part of the Skagit Gneiss Complex where they are oriented north-south to northeast-southwest (Haugerud et al., 1991; Tabor et al., 2003; Michels, 2008; Shea, 2008). Dikes in this central region record a similar extension direction and are also inconsistent with other dike swarms in the North Cascades (Fig. 29). Foliations in the southern and central Skagit Gneiss Complex also are deformed by gently northwest- or southeast-plunging folds formed between ~51 to 47 Ma (Shea, 2008).

The shallow-crustal structures of the Swauk Formation are dominated by large, generally northwest-trending folds that refold east-northeast-trending folds and by northeast-trending dikes. Extension directions recorded by the Teanaway dike swarm is slightly to moderately counterclockwise (generally ~10-20°) of the extension direction from average orientations of stretching lineations in the Skagit Gneiss Complex and the displacement direction along the Dinkelman decollement (Fig. 29). Folds in the Swauk Formation are both broadly geometrically analogous and temporally coincident with those documented in the Skagit Gneiss Complex. Top-to-the-north shear along the Dinkelman

decollement (Fig. 29) is inconsistent with southwest-northeast shortening needed to produce northwest-trending folds in both the Swauk Formation and Skagit Gneiss Complex, and the decollement has been folded by a northwest-trending fold.

The evolution of the Swauk basin, from subsidence and sediment accumulation to extension and injection of Teanaway dikes, largely reflects regional transtension that probably correlates with similar strain in the Skagit Gneiss Complex. The episode of shortening that occurred before injection of the Teanaway dikes is interpreted to result from transpression at ~51-47 Ma that also affected deeper rocks in the Skagit Gneiss Complex. Thus, both extension and shortening in the Swauk basin are reflected in the older rocks of the Skagit Gneiss Complex. These similarities imply a certain amount of structural coupling between the brittle and ductile Cascades crust during the middle Eocene. Top-to-the-north shear along the Dinkelman decollement and small rotation and inconsistent sense of extension directions between the Teanaway dikes and stretching lineations and dikes of the Skagit Gneiss Complex argue for some decoupling; whether decoupling is due to partitioning of strain to weaker ductile rocks, local influence from bounding faults, or decoupling along an unknown shear zone, remains to be seen.

CONCLUSIONS

Rapid subsidence and sediment accumulation are responsible for the >3600-m-thick Swauk Formation. The presence of at least one intraformational angular unconformity indicates tilting and erosion and that any estimate of sediment thickness is a minimum.

Folds in the Swauk Formation overall record north-northeast-south-southwest shortening, but, locally, shortening directions show considerable variability. Two generations of folds have been interpreted from bed dip reversals and strikes in map view and from cross-sections and a third generation is interpreted from map patterns of younger units. The first generation is east-northeast-trending and overprinted by the second generation of northwest-trending, larger folds. The third generation is an open, gently southeast-plunging regional syncline. Folds are moderately asymmetric with rounded hinges and formed by flexural slip. Minimum percent shortening ranges from 26% to 39%. Shortening also systematically increases toward the narrow central portion of the Swauk Formation, in part accounting for the shape of the Swauk outcrop belt. Folding is also more intense in the north toward the base of the formation, and the dip of beds shallows to the south.

The >15 km² panel of overturned beds in the central portion of the study area is part of the eastern limb of an overturned syncline. The intersection of the overturned panel and upright strata is a fault that lies between the Koppen

Mountain and Jolly Mountain transects. The fault is interpreted as a southeast-side-down normal fault or a strike-slip fault that cuts out the hinge zone of the overturned syncline.

Faults in the study area generally strike northwest. Microstructural analysis of fault rocks in the Swauk Formation indicates that there are both dextral-reverse and dextral-normal structures. Thin-section analysis of a single narrow shear zone cutting a Teanaway dike reveals dextral-reverse displacement.

The Swauk-Ingalls contact is faulted where observed in the western half of the study area and appears depositional in some locations to the east. It is generally steep ($>65^\circ$) and south-dipping.

The contact between the Swauk Formation and Teanaway Formation was largely unobserved, but it is at least locally faulted.

A $>5 \text{ km}^2$ shear zone near the northern edge of the Jolly Mountain transect is marked by concentrated shear, faulting, bedding changes, cataclastic flow, and intense grain-size reduction. No bounding faults were exposed, but approximate boundaries were traced.

The Teanaway dikes pervasively intrude the Swauk Formation. Individual dikes have a mean thickness of $\sim 16 \text{ m}$. The strikes of mean dike orientations swing from more northeast ($\sim 216^\circ$) in the western portion to more north-northeast ($\sim 197^\circ$) in the eastern portion of the study area, and record northwest-southeast extension oriented between 306° - 126° and 287° - 107° . Minimum percent

extension accommodated by the Teanaway dikes ranges from 16% to 40% in two transects.

Eocene dikes elsewhere in the central Cascades and North Cascades crystalline core are generally northeast-trending and record arc-parallel to arc-oblique extension. The dikes do show considerable variability in orientation, which suggests complex spatial changes in the Eocene strain field. Eocene dikes east of the crystalline core are north-south trending and record east-west extension. The difference in the orientation of extensional strain probably reflects the role that strike slip along the plate boundary has had in the Cascades core.

A comparison of Eocene structures in the Swauk basin with Eocene structures in deeper rocks of the Cascades core has been used to evaluate whether strain in the Eocene was coupled between deeper and shallower levels. These structures show broadly similar northeast-southwest shortening, bracketed between ~51-47 Ma, and orogen-parallel to orogen-oblique extension. However, structures in the Skagit Gneiss Complex and Swakane Gneiss record extension that appears to be slightly to moderately rotated from that of the Teanaway dikes and, in the Swakane Gneiss, the Dinkelman decollement records top-to-the-north shear that is ~70° counterclockwise from extension recorded by the Teanaway dikes. These relationships imply some decoupling between shallower and deeper-crustal rocks of the central Cascades and North Cascades core. The mechanism by which this decoupling was accommodated remains uncertain.

REFERENCES CITED

- Alexander, F., 1956, Stratigraphic and structural geology of the Blewett-Swauk area, Washington [M.S. thesis]: Seattle, University of Washington, 62 p.
- Anderson, E.M., 1951, The dynamics of faulting and dyke formation with applications to Britain, 2nd ed.: Edinburgh, Oliver and Boyd, 206 p.
- Ashleman, J.C., 1979, The geology of the western part of the Kachess Lake quadrangle, Washington [M.S. thesis]: Seattle, University of Washington, 88 p.
- Atwater, T., 1970, Implications of plate tectonics for the Cenozoic tectonic evolution of western North America: Geological Society of America Bulletin, v. 81, p. 3513-3536.
- Breitsprecher, K., Thorkelson, D.J., Groome, W.G., and Dostal, J., 2003, Geochemical confirmation of the Kula-Farallon slab window beneath the Pacific Northwest in Eocene time: Geology, v. 31, p. 351-354
- Broughton, W.A., 1944, Economic aspects of the Blewett-Cle Elum Iron Ore Zone, Chelan and Kittitas Counties, Washington: State of Washington Department of Conservation and Development, Report of Investigations, no. 12, 42 p.
- Cheney, E.S., and Hayman, N.W., 2009, The Chiwaukum Structural Low: Cenozoic shortening of the central Cascade Range, Washington State, USA: Geological Society of America Bulletin, v. 121, p. 1135-1153.

- Clayton, D.N., 1973, Volcanic history of the Teanaway Basalt, east-central Cascade Mountains, Washington [M.S. thesis]: Seattle, University of Washington, 55 p.
- Doran, B.A., Miller, R.B., and Michels, Z., 2007, Structure and implications of Eocene dike swarms in Washington Cascades: Geological Society of America Abstracts with Programs, v. 39, no. 4, p. 10.
- Dostal, J., Breitsprecher, K., Church, B.N., Thorkelson, D., and Hamilton, T.S., 2003, Eocene melting of Precambrian lithospheric mantle: Analcime-bearing volcanic rocks from the Challis-Kamloops belt of south central British Columbia: Journal of Volcanology and Geothermal Research, v. 126, p. 303-326.
- Dragovich, J.D., Logan, R.L., Schasse, H.W., Walsh, T.J., Lingley, W.S., Jr., Norman, D.K., Gerstel, W.J., Lapen, T.J., Schuster, J.E., and Meyers, K.D., 2002, Geologic map of Washington; northwest quadrant: Washington Department of Natural Resources, Division of Geology and Earth Resources, scale 1:250,000, 1 sheet.
- Ellis, R.C., 1959, The geology of the Dutch Miller Gap area [Ph.D. thesis]: Seattle, University of Washington, 112 p.
- Engebretson, D.C., Cox, A., and Gordon, R.G., 1985, Relative motion between oceanic and continental plates in the Pacific basin: Geological Society of America Special Paper 206, 58 p.

- Evans, J.E., and Johnson, S.Y., 1989, A field guide to the Paleogene strike-slip basins of Central Washington: Swauk Formation and Chumstick Formation, *in* Joseph, N.L., et al., eds., Geologic guidebook for Washington and adjacent areas: Washington Division of Geology and Earth Resources Information Circular 86, p. 213-237.
- Evans, J.E., 1994, Depositional history of the Eocene Chumstick Formation: Implications of tectonic partitioning for the history of the Leavenworth and Entiat-Eagle Creek fault systems, Washington: *Tectonics*, v. 13, p. 1425-1444.
- Foster, R.J., 1958, The Teanaway dike swarm of Central Washington: *American Journal of Science*, v. 256, p. 644-653.
- Foster, R.J., 1960, Tertiary geology of a portion of the Central Cascade Mountains, Washington: *Geological Society of America Bulletin*, v. 71, p. 99-125.
- Frizzell, V.A., Jr., 1979, Petrology and stratigraphy of Paleogene nonmarine sandstones, Cascade Range, Washington: U.S. Geological Survey Open-File Report 79-1149, 151p.
- Gresens, R.L., Naeser, C.W., and Whetten, J.T., 1981, Stratigraphy and age of the Chumstick and Wenatchee formations; Tertiary fluvial and lacustrine rocks, Chiwaukum Graben, Washington: *Geological Society of America Bulletin* v. 92, Part II, p. 223-236.

- Haugerud, R.A., Van der Heyden, P., Tabor, R.W., Stacey, J.S., and Zartman, R.E., 1991, Late Cretaceous and early Tertiary plutonism and deformation in the Skagit Gneiss Complex, North Cascade Range, Washington and British Columbia: Geological Society of America Bulletin, v. 103, p. 1297-1307.
- Johnson, S.Y., 1984, Evidence for a margin-truncating transcurrent fault (pre-late Eocene) in western Washington: *Geology*, v. 12, p. 538-341.
- Johnson, S.Y., 1985, Eocene strike-slip faulting and nonmarine basin formation in Washington, *in* Biddle, K.T., and Christie-Blick, N., eds., Society of Economic Paleontologists and Mineralogists Special Publication, no. 37, p. 283-302.
- Klausen, M.B., 2006, Similar dyke thickness variation across three volcanic rifts in the North Atlantic region: Implications for intrusion mechanisms: *Lithos*, v. 92, p. 137-153.
- Lamey, C.A., and Hotz, P.E., 1952, The Cle Elum River nickeliferous iron deposits, Kittitas County, Washington: U.S. Geological Survey Bulletin, v. 41, p. 27-67.
- Lupher, R.L., 1944, Stratigraphic aspects of the Blewett-Cle Elum iron ore zone, Chelan and Kittitas counties, Washington: State of Washington Department of Conservation and Development, Report of Investigations, no. 11, 63 p.

- MacDonald, J.H., Jr., Harper, G.D., Miller, R.B., Miller, J.S., Mlinarevic, A.N., and Schultz, C.E., 2008, The Ingalls ophiolite complex, central Cascades, Washington: Geochemistry, tectonic setting, and regional correlations, *in* Wright, J.E., and Shervais, J.W., eds., *Ophiolites, arcs, and batholiths: A tribute to Cliff Hopson*: Geological Society of America Special Paper 438, p. 133-160.
- Matzel, J.E.P., Bowring, S.A., and Miller, R.B., 2006, Time scales of pluton construction at differing crustal levels; examples from the Mount Stuart and Tenpeak Intrusions, north Cascades, Washington: Geological Society of America Bulletin, v. 118, p. 1412-1430.
- Madsen, J.K., Thorkelson, D.J., Friedman, R.M., and Marshall, D.D., 2006, Cenozoic to Recent plate configurations in the Pacific Basin: Ridge subduction and slab window magmatism in western North America: *Geosphere*, v. 2, p. 11-34.
- McCarley Holder, G.A., Holder, R.W., and Carlson, D.H., 1990, Middle Eocene dike swarms and their relation to contemporaneous plutonism, volcanism, core-complex mylonitization, and graben subsidence, Okanogan Highlands, Washington: *Geology*, v. 18, p. 1082-1085.
- McGroder, M.F., 1991, Reconciliation of two-sided thrusting, burial metamorphism, and diachronous uplift in the Cascades of Washington and British Columbia: Geological Society of America Bulletin, v. 103, p. 189-209.

- Mendoza, M., 2008, Tectonic implications of Eocene Teanaway dike swarm in the eastern Swauk basin, central Washington: Geological Society of America Abstracts with Programs, v. 40, no. 1, p. 66.
- Miller, R.B., 1985, The ophiolitic Ingalls Complex, north-central Cascade Mountains, Washington: Geological Society of America Bulletin, v. 96, p. 27-42.
- Miller, R.B., and Bowring, S.A., 1990, Structure and chronology of the Oval Peak batholith and adjacent rocks: Implications for the Ross Lake fault zone, North Cascades, Washington: Geological Society of America Bulletin, v. 102, p. 1361-1377.
- Miller, R.B., Brown, E.H., McShane, D.P., and Whitney, D.L., 1993, Intra-arc crustal loading and its tectonic implications, North Cascades crystalline core, Washington and British Columbia: Geology, v. 21, p. 255-258.
- Miller, R.B., Matzel, J.P., Paterson, S.R., and Stowell, H., 2003, Cretaceous to Paleogene Cascades arc: Structure, metamorphism, and timescales of magmatism, burial, and exhumation of a crustal section, *in* Swanson, T.W., ed., Western Cordillera and Adjacent Areas. Boulder, Colorado, Geological Society of America Field Guide, p. 107-135.
- Miller, R.B., and Paterson, S.R., 2001, Influence of lithological heterogeneity, mechanical anisotropy, and magmatism on the rheology of an arc, North Cascades, Washington: Tectonophysics, v. 342, p. 351-370.

- Miller, R.B., Paterson, S.R., Lebit, H., Alsleben, H., Luneburg, C., 2006, Significance of composite lineations in the mid- to deep crust: a case study from the North Cascades, Washington: *Journal of Structural Geology*, v. 28, p. 302-322.
- Misch, P., 1966, Tectonic evolution of the northern Cascades of Washington State—a west Cordilleran case history: *Canadian Institute of Mining and Metallurgy, Special Volume 8*, p. 101-148.
- Misch, P., 1977, Dextral displacements at some major strike faults in the North Cascades: *Geological Association of Canada Abstracts with Programs*, v. 2, p. 37.
- Michels, Z.D., 2008, Structure of the central Skagit Gneiss Complex, North Cascades, Washington [M.S. thesis]: San Jose, San Jose State University, 95 p.
- Paterson, S.R., Miller, R.B., Alsleben, H., Whitney, D.L., Valley, P.M., and Hurlow, H., 2004, Driving mechanisms for >40 km of exhumation during contraction and extension in a continental arc, Cascades core, Washington: *Tectonics*, v. 23, TC3005, doi: 10.1029/2002TC001440.
- Peters, R.L., and Tepper, J.H., 2006, Petrology of the Teanaway dike swarm, central Cascades, Washington: *Geological Society of America Abstracts with Programs*, v. 38, no. 5, p. 9.

- Raviola, F.P., 1988, Metamorphism, plutonism and deformation in the Pateros-Altas Lake region, north-central Washington [M.S. thesis]: San Jose, San Jose State University, 181 p.
- Robin, P., and Cruden, A.R., 1994, Strain and vorticity patterns in ideally ductile transpression zones: *Journal of Structural Geology*, v. 16, p. 447-466.
- Russell, I.C., 1900, A preliminary paper on the geology of the Cascade Mountains in northern Washington: United States Geological Survey Annual Report 20, Part 2, p. 83-210.
- Sanderson, D.J., and Marchini, W.R., 1984, Transpression: *Journal of Structural Geology*, v. 6, p. 449-458.
- Shea, E.K., 2008, Structure of the southern Skagit Gneiss Complex, North Cascades, Washington [M.S. thesis]: San Jose, San Jose State University, 90 p.
- Smith, G.O., and Willis, B., 1901, The Cle Elum iron-ores, Washington: American Institute of Mining, Metallurgical and Petroleum Engineers, Transactions, v. 30, p. 356-366.
- Smith, G.O., 1904, Description of the Mount Stuart quadrangle, Washington: U.S. Geological Survey, Geologic Atlas, Folio 106, 10 p.
- Smith, G.O., and Calkins, F.C., 1906, Description of the Snoqualmie quadrangle [Washington]: U.S. Geological Survey, Geologic Atlas, Folio 139, 14 p.
- Tabor, R.W., Waitt, R.B., Jr., Frizzell, V.A., Jr., Swanson, D.A., Byerly, G.R., and Bentley, R.D., 1982, Geologic map of the Wenatchee quadrangle,

Washington: U.S. Geological Survey Miscellaneous Investigations map MI-1311, scale 1:100,000, 1 sheet, 31 p. text.

Tabor, R.W., Frizzell, V.A., Jr., Vance, J.A., and Naeser, C.W., 1984, Ages and stratigraphy of lower and middle Tertiary sedimentary and volcanic rocks of the Central Cascades, Washington: Applications to the tectonic history of the Straight Creek fault: Geological Society of America Bulletin, v. 95, p. 26-44.

Tabor, R.W., Frizzell, V.A., Jr., Whetten, J.T., Waitt, R.B., Swanson, D.A., Byerly, G.R., Booth, D.B., Hetherington, M.J., and Zartman, R.E., 1987, Geologic map of the Chelan 30-minute by 60-minute quadrangle, Washington: U.S. Geological Survey Geologic Investigation Series, I-1661, scale 1:100,000, 1 sheet, 56 p. text.

Tabor, R.W., Haugerud, R.A., and Miller, R.B., 1989, Overview of the geology of the North Cascades: International Geological Congress Trip T307, American Geophysical Union, 62 p.

Tabor, R.W., Frizzell, V.A., Jr., Booth, D.B., and Waitt, R.B., 2000, Geologic map of the Snoqualmie Pass 30x60 minute quadrangle, Washington: U.S. Geological Survey Geologic Investigations map MI-2538, scale 1:100,000, 1 sheet, 57 p. text.

Tabor, R.W., Haugerud, R.A., Hildreth, W., and Brown, E.H., 2003, Geologic map of the Mount Baker 30- by 60-minute quadrangle, Washington: U.S.

Geological Survey, Geologic Investigation Series, I-2660, scale 1:100,000,
1 sheet, 70 p. text.

Taylor, S.B., 1985, Stratigraphy, sedimentology, and paleogeography of the
Swauk Formation in the Liberty area, central Cascades, Washington [M.S.
thesis]: Pullman, Washington State University, 199 p.

Taylor, S.B., Johnson, S.Y., Fraser, G.T., and Roberts, J.W., 1988,
Sedimentation and tectonics of the lower and middle Eocene Swauk
Formation in eastern Swauk Basin, central Cascades, central Washington:
Canadian Journal of Earth Sciences, v. 25, p. 1020-1036.

Tepper, J.H., Nelson, B.K., Clark, K., and Barnes, R.P., 2008, Heterogeneity in
mantle sources for Eocene basalts in Washington: Trace element and Sr-
Nd isotopic evidence from the Crescent and Teanaway basalts: American
Geophysical Union Abstracts with Programs, v. 41, abstract no. 2121.

Thorkelson, D.J., 1995, Subduction of diverging plates and the principles of slab
window formation: Tectonophysics, v. 255, p. 47-63.

Tikoff, B., and Teyssier, C., 1994, Strain modeling of displacement-field
partitioning in transpressional orogens: Journal of Structural Geology, v.
16, p. 1575-1588

Twiss, R.J., and Moores, E.M., 1992, Structural geology: New York, W.H.
Freeman and Company, 532 p.

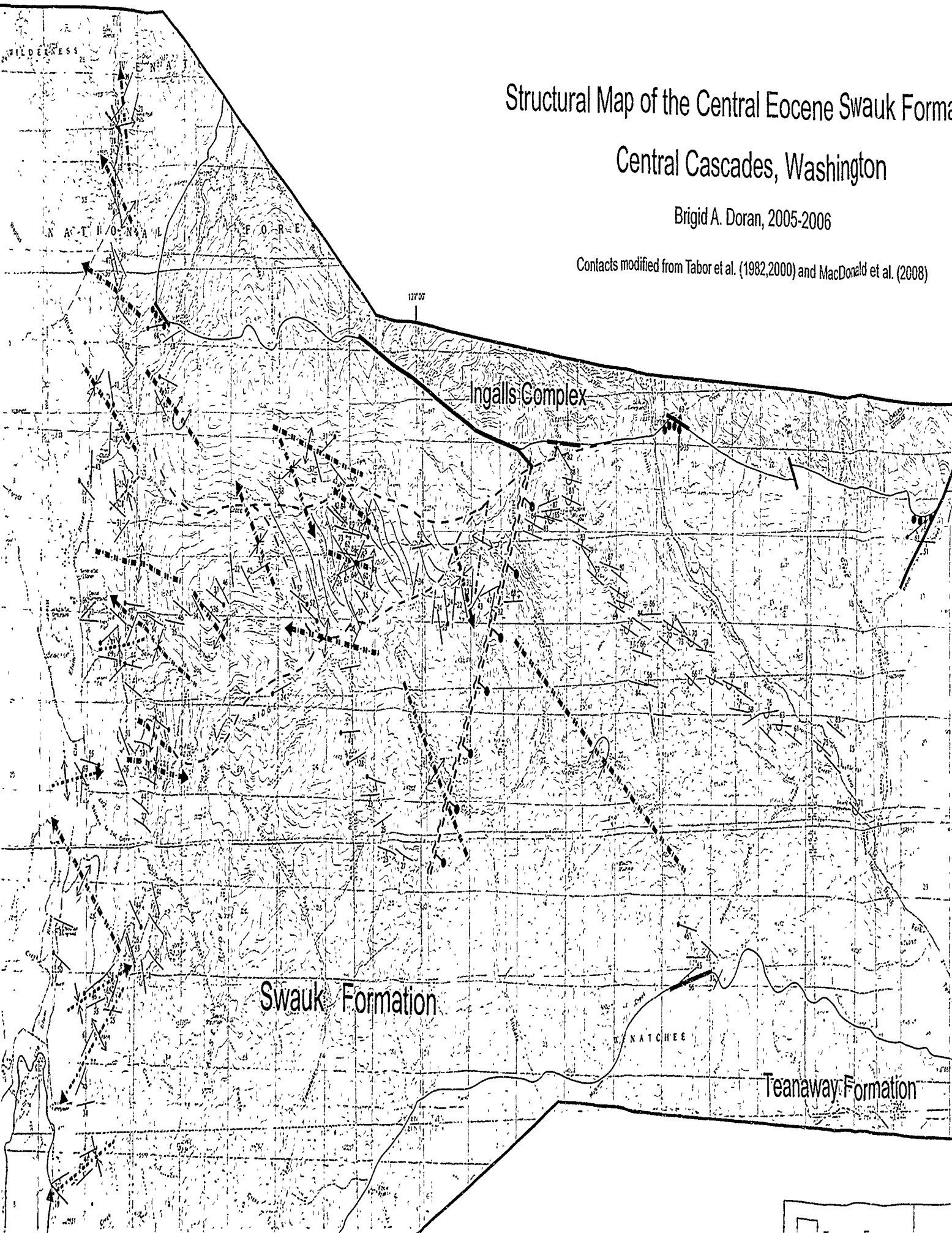
Vance, J.A., and Miller, R.B., 1981, The movement history of the Straight Creek
fault in Washington State, *in* Monger, J.W.H., ed, The last 100 million

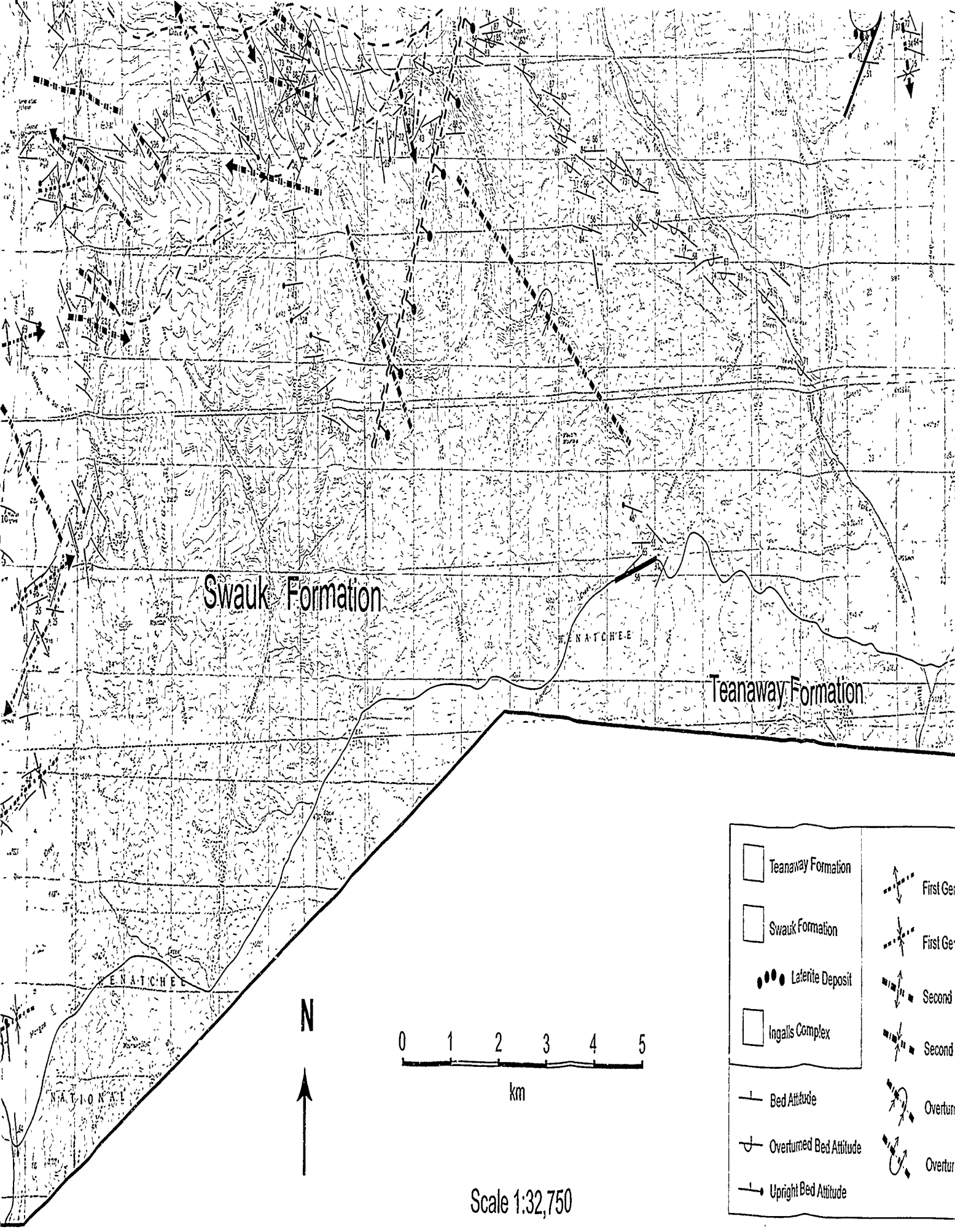
- years (mid-Cretaceous to Holocene) of geology and mineral deposits in the Canadian Cordillera: Cordilleran Section Geological Society of Canada, Program and Abstracts for 1981 meeting, Vancouver, p. 39-41.
- Vance, J.A., and Miller, R.B., 1983, Geologic constraints on the movement history of the Straight Creek fault, *in* Yount, J.C., ed., Proceedings of workshop XIV; Earthquake hazards of the Puget Sound region, Washington: U.S. Geological Survey Open-file Report 83-19, p. 302-306.
- Wilcox, R.E., Harding, T.P., and Seely, D.R., 1973, Basic wrench tectonics: American Association of Petroleum Geologists Bulletin, v. 57, p. 74-96.
- Wells, R.E., Engebretson, D.C., Snively, P.D., Jr., and Coe, R.S., 1984, Cenozoic plate motions and the volcano-tectonic evolution of western Oregon and Washington: Tectonics, v. 3, p. 275-294.
- Wernicke, B.P., and Getty, S.R., 1997, Intracrustal subduction and gravity currents in the deep crust; Sm-Nd, Ar-Ar, and thermobarometric constraints from the Skagit Gneiss Complex, Washington: Geological Society of America Bulletin, v. 109, p. 1149-1166.
- Winter, J.D., 2001, An introduction to igneous and metamorphic petrology: New Jersey, Prentice Hall, 697 p.
- Zoback, M.D., Zoback, M.L., Mount, V.S., Suppe, J., Eaton, J.P., Healy, J.H., Oppenheimer, D., Reasenber, P., Jones, L., Raleigh, C.B., Wong, I.G., Scotti, O., and Wentworth, C., 1987, New evidence on the state of stress of the San Andreas fault system: Science, v. 238, p. 1105-1110.

Structural Map of the Central Eocene Swauk Formation Central Cascades, Washington

Brigid A. Doran, 2005-2006

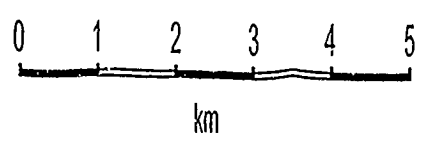
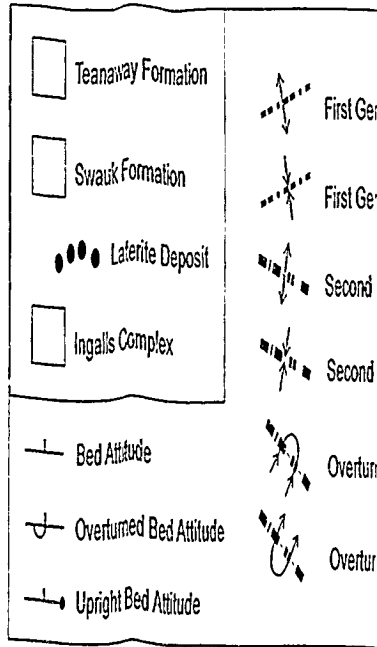
Contacts modified from Tabor et al. (1982,2000) and MacDonald et al. (2008)





Swauk Formation

Teanaway Formation

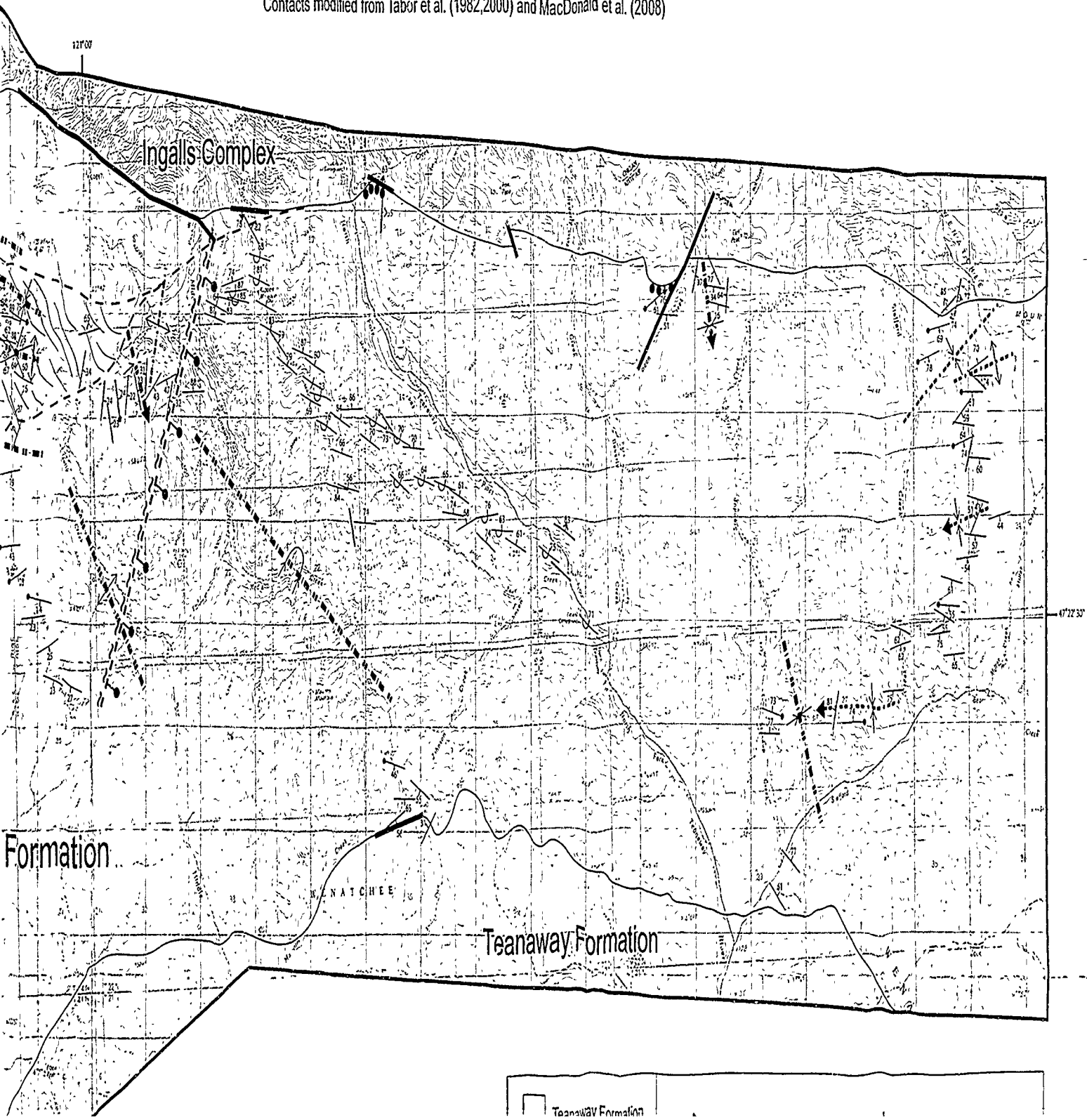


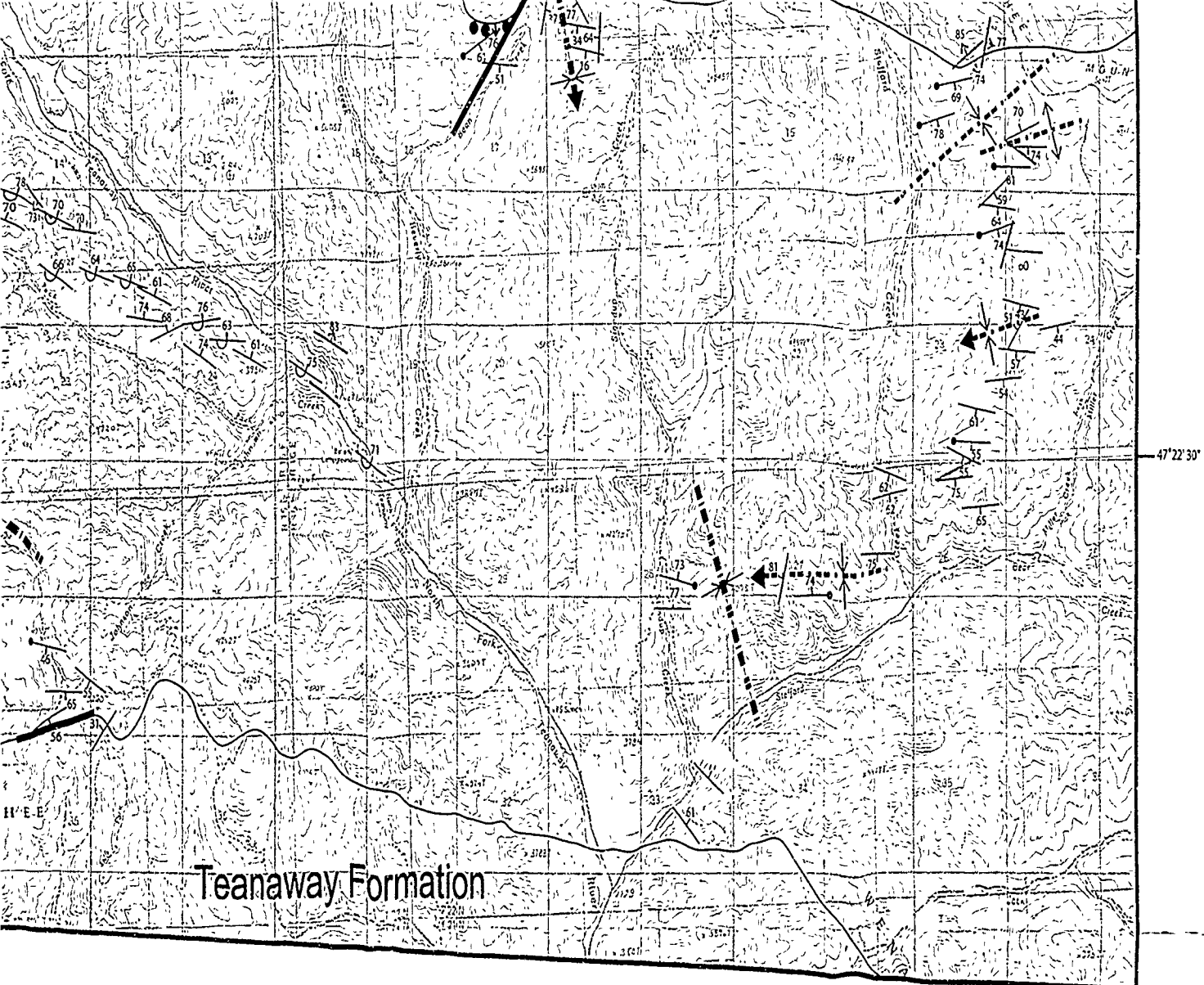
Scale 1:32,750

Structural Map of the Central Eocene Swauk Formation, Central Cascades, Washington

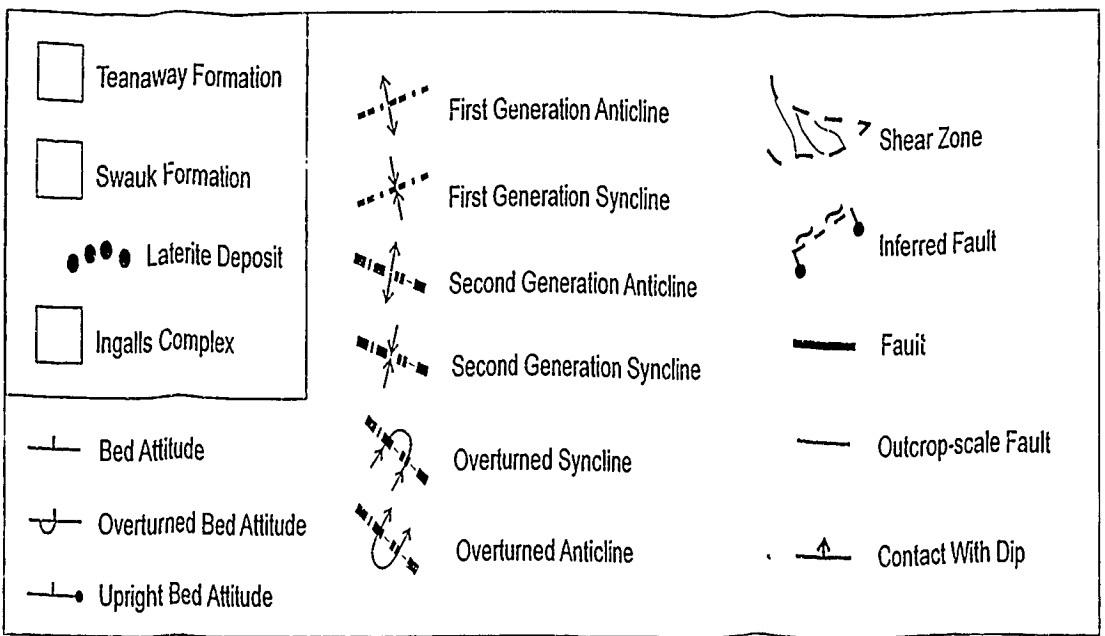
Brigid A. Doran, 2005-2006

Contacts modified from Tabor et al. (1982,2000) and MacDonald et al. (2008)





Teaway Formation



5